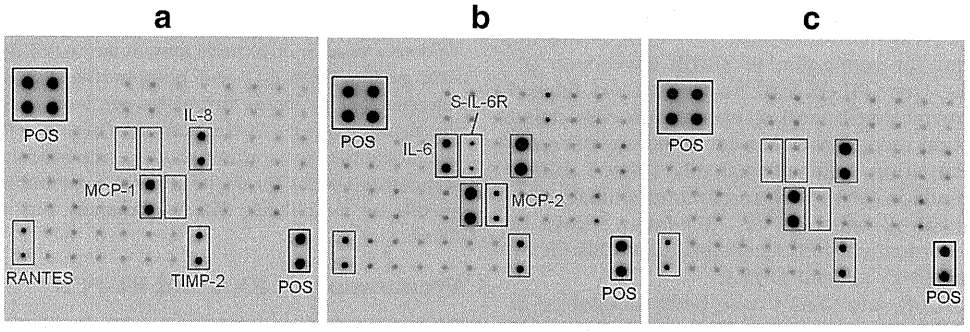

FIGURE 1. Antibody array of culture supernatants from corneal fibroblasts stimulated by the supernatant of necrotic corneal epithelial cells. Culture supernatant from corneal fibroblasts was analyzed with an antibody array (Human Inflammation Antibody III kit; Ray Biotech Inc.). Representative arrays analyzing culture supernatant obtained from corneal fibroblasts are shown in (**a**). Cells cultured with serum-free medium. (**b**) Cells cultured with serum free medium containing the supernatant of necrotic corneal epithelial cell. (**c**) Cells cultured with serum free medium containing the supernatant of necrotic corneal epithelial cells and human IL-1 receptor antagonist (IL-1RA: 100 ng/mL).

allowed to stand overnight at 4°C. After three washes in PBS, the slides were incubated for 40 minutes with FITC-conjugated donkey anti-goat IgG pAb (1:100 dilution) at room temperature. After being washed three more times with PBS, the slides were incubated for 2 hours with rabbit anti-S100 A4 pAb (ready-to-use) at room temperature. After three washes in PBS, the slides were incubated for 40 minutes with biotinylated goat anti-rabbit pAb (1:300 dilution) at room temperature. After being washed in PBS, the slides were incubated for 40 minutes with fluorescent dye-conjugated (Alexa Fluor 594; Invitrogen) streptavidin. Counterstaining was done with 4′,6′-diamidino-2-phenindole (DAPI). The slides were then inspected by the use of a laser confocal microscope (TCS SP5; Leica Microsystems, Tokyo, Japan).

Statistical Analysis

Results were expressed as the mean ± SE. Differences were evaluated by Student's *t*-test using analytical software (Excel; Microsoft, Redmond, WA).

RESULTS

Chemokine and Cytokine Production by Corneal Fibroblasts Is Stimulated by Supernatant of Necrotic Corneal Epithelial Cells

Representative arrays analyzing culture supernatant obtained from corneal fibroblasts are shown in Figure 1. We estimated the mean optical intensity of positive spots from the culture supernatants (Fig. 2). Corneal fibroblasts cultured with serum-free medium constitutively produced IL-8, MCP-1, RANTES (Regulated upon Activation, Normal T Expressed, and presumably Secreted), and TIMP-2 (Fig. 1a). Moreover, production of IL-6, MCP-2, and SIL-6R was induced and production of IL-8, MCP-1, and RANTES was enhanced when corneal fibroblasts were cultured with serum-free medium containing the supernatant of necrotic corneal epithelial cells (Fig. 1b). Among these molecules, IL-6 was most strongly induced by the supernatant of necrotic corneal epithelial cells (Fig. 2).

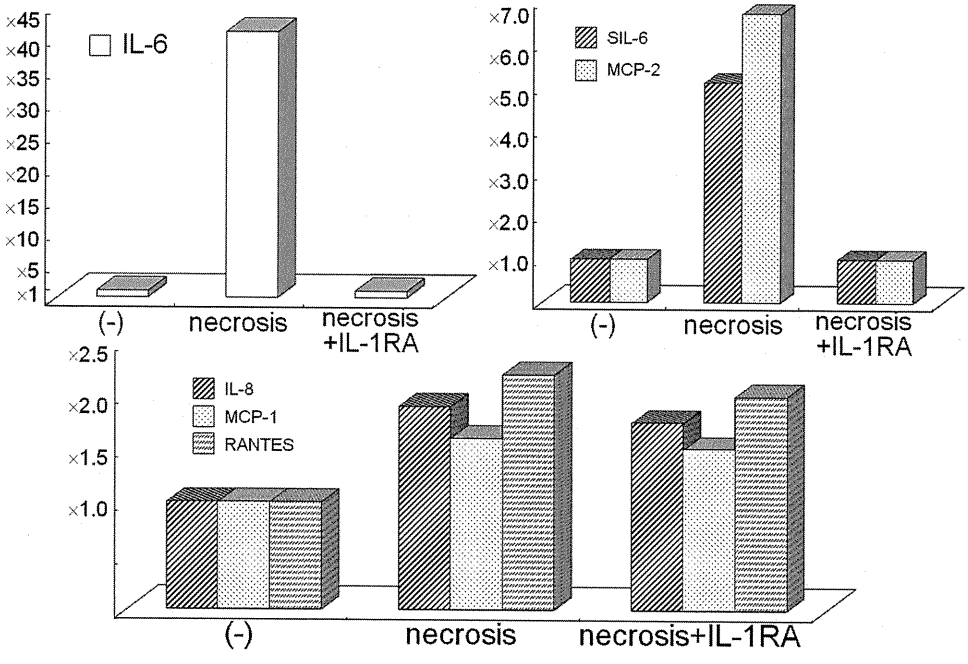

FIGURE 2. Estimation of the mean optical intensity of positive spots from the culture supernatants. Corneal fibroblasts constitutively produced IL-8, MCP-1, RANTES, and TIMP-2. When cells were cultured with the supernatant of necrotic corneal epithelial cells, the production of IL-6, MCP-2, and SIL-6R was induced and that of IL-8, MCP-1, and RANTES was enhanced. Treatment with an IL-1RA almost completely inhibited the production of IL-6, MCP-2, and SIL-6R and partially inhibited the production of IL-8, MCP-1, and RANTES.

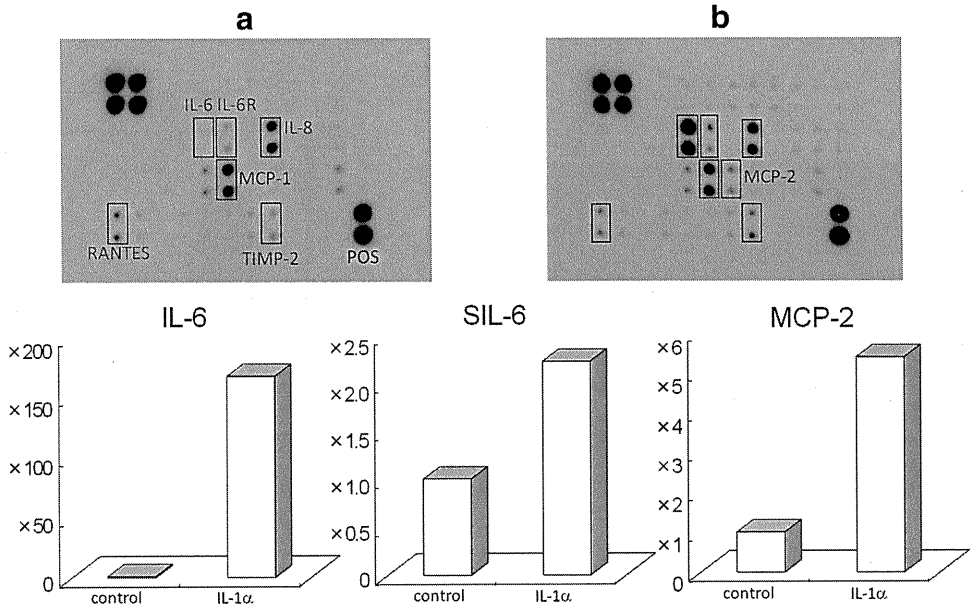

FIGURE 3. Antibody array of culture supernatants from corneal fibroblasts stimulated by recombinant IL-1α. Culture supernatant from corneal fibroblasts treated with recombinant human IL-1α (30 ng/mL) was analyzed with a commercial antibody array. Representative arrays analyzing culture supernatant are shown: (**a**) Cells cultured with serum-free medium. (**b**) Cells cultured with serum-free medium with recombinant IL-1α (30 ng/mL). The mean optical intensity of positive spots was estimated from the culture supernatants. Corneal fibroblasts constitutively produced IL-8, MCP-1, RANTES, and TIMP-2. When cells were treated with IL-1α, the production of IL-6, SIL-6R, and MCP-2 was induced. Among these molecules, IL-6 was most strongly induced by IL-1α.

Next, we investigated which factor in the supernatant of necrotic corneal epithelial cells induced the production of IL-6, MCP-2, and SIL-6R by corneal fibroblasts. Treatment with an IL-1R antagonist almost completely inhibited the production of these molecules, indicating that IL-1 derived from necrotic corneal epithelial cells induced the production of IL-6, MCP-2, and SIL-6R by corneal fibroblasts. On the other hand, the IL-1R antagonist partially inhibited production of IL-8, MCP-1, and RANTES by corneal fibroblasts cultured with the supernatant of necrotic corneal epithelial cells, indicating that other danger molecules also enhanced the production of these chemokines (Figs. 1c, 2).

Influence of IL-1α on IL-6 Production by Corneal Fibroblasts

The mean optical density of positive spots obtained from the culture supernatants of cells treated with IL-1α (30 ng/mL, 24 hours) was compared with that of spots from the supernatants of untreated cells (Fig. 3), revealing that stimulation of fibroblasts with IL-1α induced the production of IL-6, MCP-2, and SIL-6R. Among these molecules, IL-6 was most strongly induced by IL-1α.

IL-6R and gp130 Expression by Corneal Fibroblasts

Corneal fibroblasts showed the expression of mRNAs for mIL-6R and DS-SIL-6R by RT-PCR (Fig. 4). However, when cell surface expression of mIL-6R and gp130 proteins on corneal fibroblasts was examined by flow cytometry, expression of mIL-6R was not detected, but gp130 was detected. This result indicates that corneal fibroblasts showed little or no cell surface expression of mIL-6R.

IL-6R and gp130 Expression by Corneal Epithelial Cells

Corneal epithelial cells showed the expression of mRNAs for mIL-6R and DS-SIL-6R by RT-PCR (Fig. 5). When cell surface expression of mIL-6R and gp130 proteins on corneal epithelial cells was examined by flow cytometry, both proteins on corneal epithelial cells were detected almost equally.

Expression of Phosphorylated STAT3 by Corneal Fibroblasts

We examined the influence of IL-6, SIL-6R, or IL-6/SIL-6R on phosphorylation of STAT3 in corneal fibroblasts. Figure 6 reveals that IL-6 alone increased STAT3 phosphorylation at a high dose, whereas SIL-6R alone did not induce the phosphorylation of STAT3. On the other hand, the IL-6/SIL-6R significantly increased STAT3 phosphorylation.

VEGF and MCP-1 Production by Corneal Fibroblasts

When we examined the production of VEGF by corneal fibroblasts, IL-6 or SIL-6R alone did not induce VEGF production. On the other hand, the IL-6/SIL-6R significantly induced VEGF production (Fig. 7A). We also examined MCP-1 production by corneal fibroblasts. We found that IL-6 or SIL-6R alone slightly induced the production of MCP-1, whereas IL-6/SIL-6R significantly induced its production (Fig. 7B).

Expression of Phosphorylated STAT3 by Corneal Epithelial Cells

We examined the effect of IL-6, SIL-6R, or IL-6/SIL-6R on phosphorylation of STAT3 in corneal epithelial cells. As shown in Figure 8, IL-6 alone and the IL-6/SIL-6R significantly increased the expression of phosphorylated STAT3 in corneal epithelial cells, but SIL-6R alone did not increase its expression.

Corneal Epithelial Cell Migration in the Scratch Assay

The scratch assay was done to assess in vitro migration of cultured corneal epithelial cells stimulated by IL-6, SIL-6R, or IL-6/SIL-6. Figure 9 shows that IL-6 or IL-6/SIL-6R significantly induced cell migration compared with that by untreated cells. Surprisingly, SIL-6R alone also induced the migration of these cells.

Immunohistochemistry

We observed the expression of IL-6R and S100 A4 in corneal fibroblasts at 24 hours after corneal injury. S100 A4 is the marker of activated corneal fibroblasts.[35] Corneal fibroblasts at and nearby the site of injury were stained with an antibody

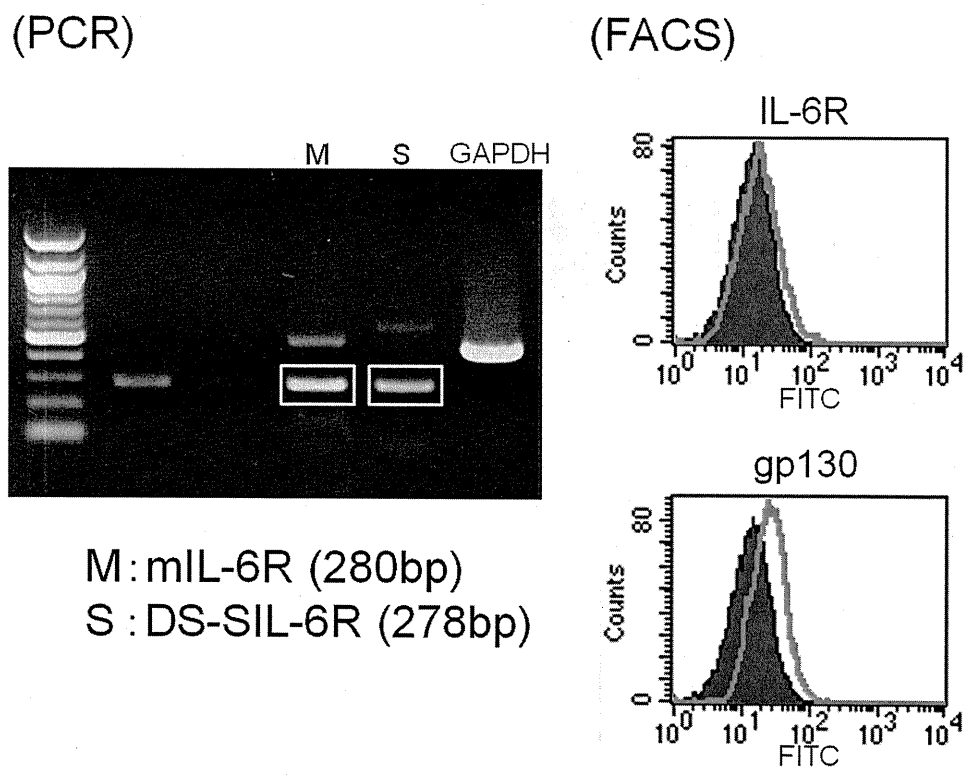

FIGURE 4. Expression of IL-6R and gp130 on primary cultured corneal fibroblasts. Corneal fibroblasts showed strong expression of the mRNAs for mIL-6R (280 bp) and DS-SIL-6R (278 bp) by RT-PCR. Next, the expression of mIL-6R and gp130 on corneal fibroblasts by flow cytometry was examined. mIL-6R was not expressed, but gp130 was expressed on the cell surface of corneal fibroblasts (*black line*, control mAb; *green line*, anti-IL-6R mAb or anti-gp130 mAb).

against IL-6R together with S100 A4 antibody. Immunostaining for IL-6R was also recognized in basal cells of the epithelium near the site of injury. There was no immunostaining for IL-6R and S100 A4 in keratocytes or corneal epithelial cells of the intact mouse cornea (data not shown). These immunohistochemical analyses (Fig. 10) for mouse corneal wound healing model showed IL-6R expression on activated fibroblasts.

DISCUSSION

This study showed that culture supernatant derived from necrotic corneal epithelial cells induced the production of IL-6, MCP-2, and SIL-6R by corneal fibroblasts, whereas an IL-1R antagonist inhibited the production of these molecules almost completely. In addition, recombinant IL-1α induced the pro-

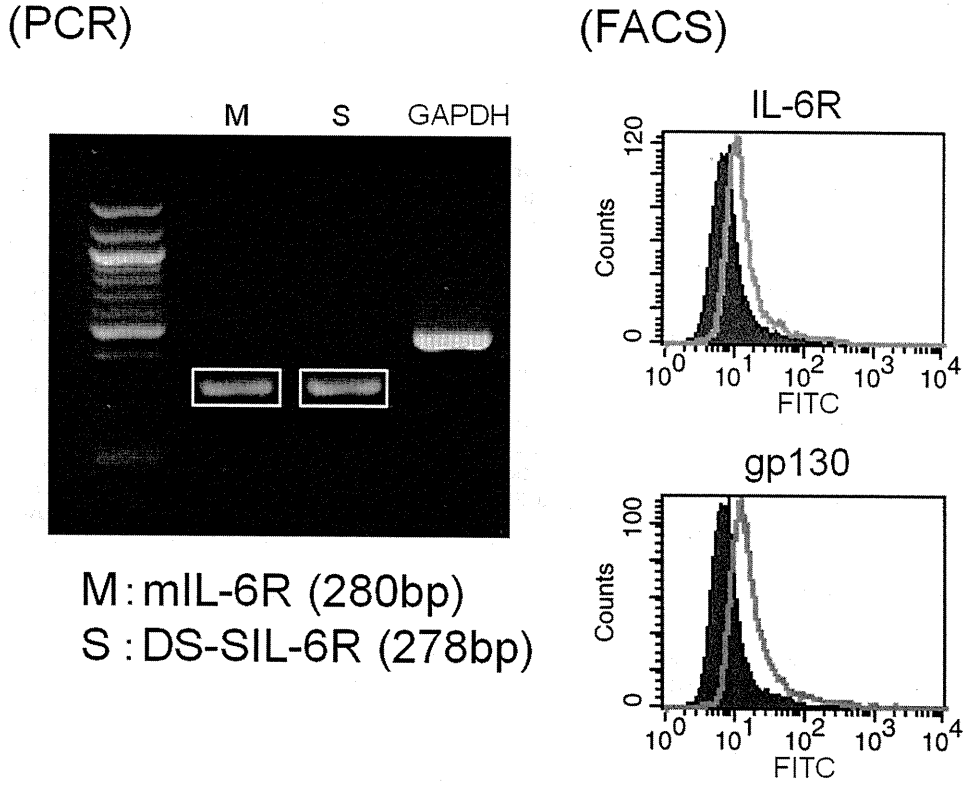

FIGURE 5. Expression of IL-6R and gp130 on primary cultured corneal epithelial cells. Corneal epithelial cells showed strong expression of the mRNAs for mIL-6R (280 bp) and DS-SIL-6R (278 bp) by RT-PCR. Next, the expression of mIL-6R and gp130 on corneal epithelial cells by flow cytometry was examined. Both mIL-6R and gp130 were expressed on the cell surface of corneal epithelial cells (*black line*, control mAb; *green line*, anti-IL-6R mAb or anti-gp130 mAb).

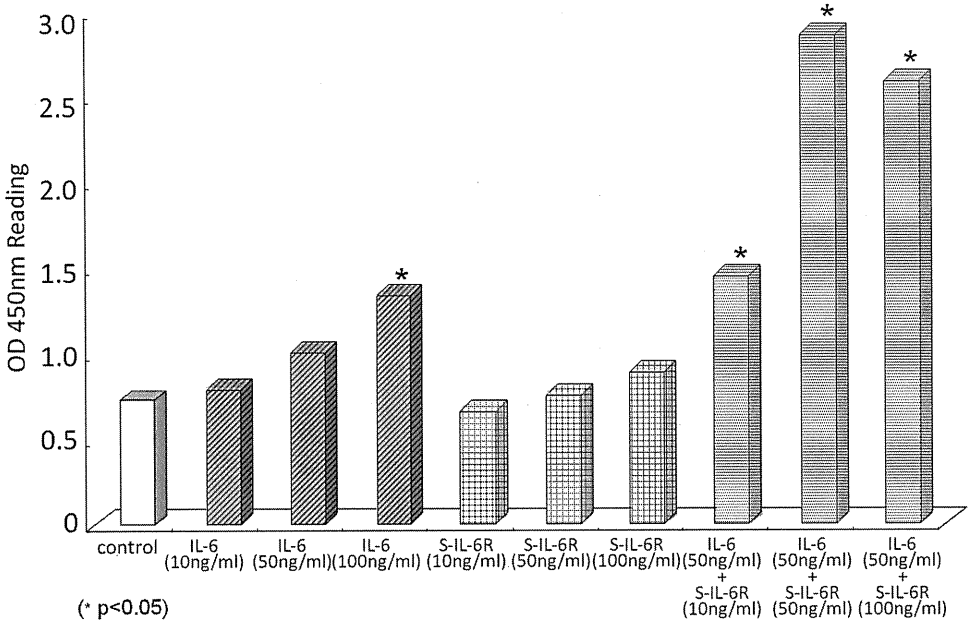

FIGURE 6. Expression of phosphorylated STAT3 by corneal fibroblasts. The influence of IL-6, SIL-6R, or IL-6/SIL-6R on phosphorylation of STAT3 was examined by ELISA. IL-6 alone increased STAT3 phosphorylation at a high dose (100 ng/mL), whereas SIL-6R alone did not induce the phosphorylation. IL-6/SIL-6R significantly increased STAT3 phosphorylation.

duction of IL-6, MCP-2, and SIL-6R. These results demonstrate that IL-1 derived from necrotic corneal epithelial cells stimulates corneal fibroblasts via IL-1R, resulting in the production of IL-6, MCP-2, and SIL-6R. Necrotic corneal epithelial cell supernatant also enhanced the production of IL-8, MCP-1, and RANTES, whereas the IL-1R antagonist partially inhibited their production, suggesting that other endogenous danger molecules influenced production of these chemokines in addition to IL-1. Among these various molecules, IL-6 may be the key molecule for sterile inflammation of the cornea and corneal wound healing. Sotozono et al.[36] showed that IL-1α and IL-6 levels are dramatically elevated in the regenerating epithelium of the mouse cornea during the early stage of recovery from an alkali burn. Biswas et al.[37] demonstrated that herpes infection of the cornea induced the expression IL-1α and IL-6 in mice. These results indicate that chemical injury or viral infection of cornea induces the release of IL-1α from damaged corneal epithelial cells, enhances IL-6 production by corneal fibroblasts, and promotes inflammatory cell infiltration into the corneal stroma.

Cellular responses to IL-6 or the IL-6/SIL-6R complex are determined by the level of IL-6R expression. The level of ubiquitously expressed gp130 protein is believed to be relatively constant for all cells, whereas expression of IL-6R varies between different cell types. Cells that do not have surface expression of IL-6R can be stimulated only by the IL-6/SIL-6R complex (the trans-signaling pathway) and are insensitive to IL-6 alone. Cells with fewer IL-6R molecules on their surface than gp130 molecules can respond to IL-6, and this response

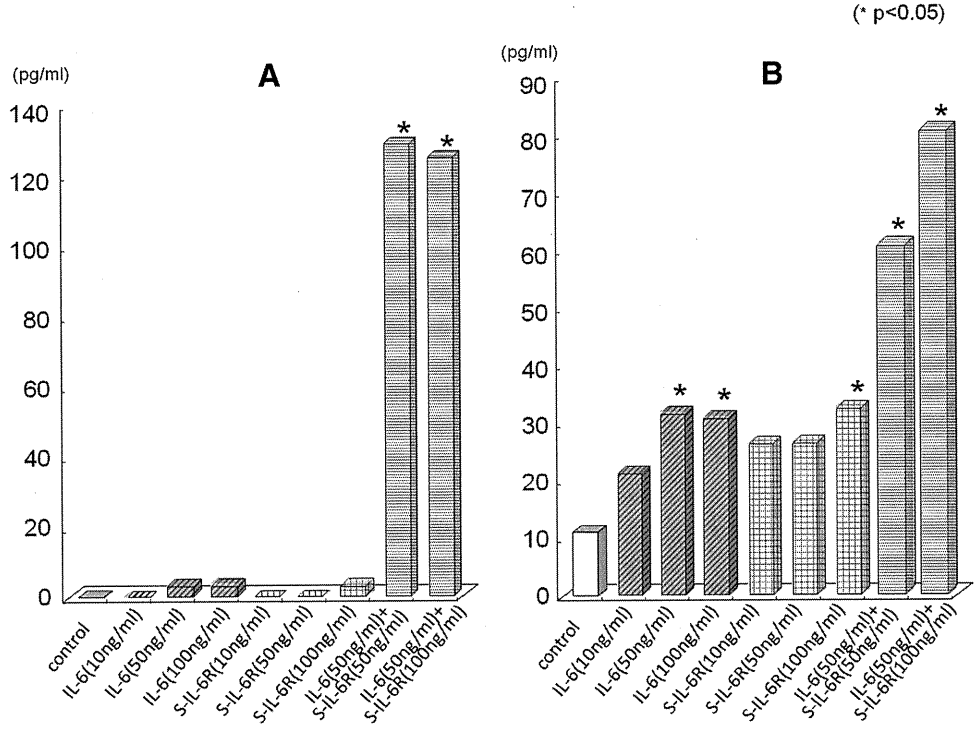

FIGURE 7. VEGF and MCP-1 production by corneal fibroblasts. The production of VEGF and MCP-1 by corneal fibroblasts was examined by ELISA. IL-6 or SIL-6R alone did not induce VEGF production. The IL-6/SIL-6R significantly induced VEGF production (**A**). IL-6 or SIL-6R alone slightly induced the production of MCP-1, whereas the IL-6/SIL-6R significantly induced its production (**B**).

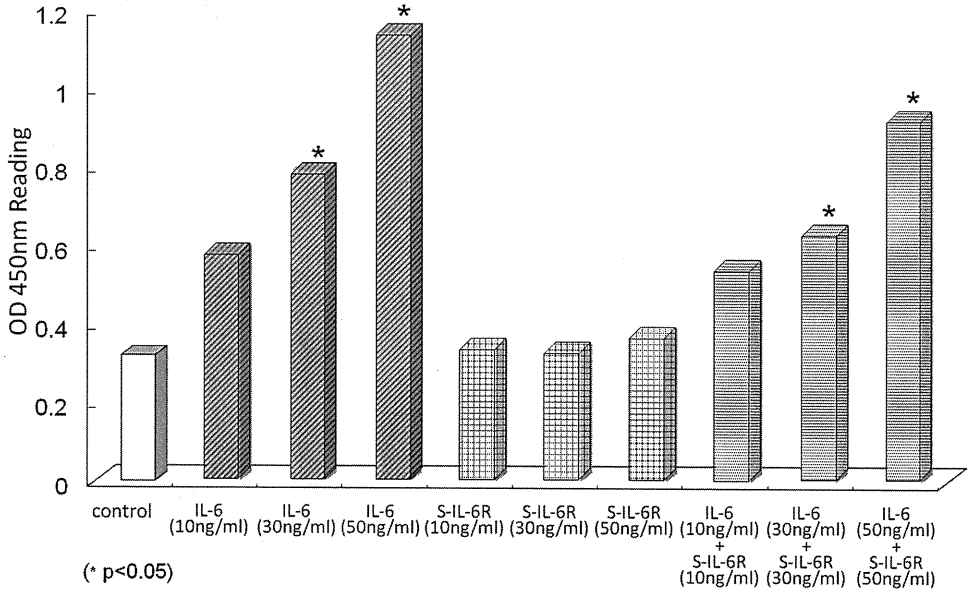

FIGURE 8. Expression of phosphorylated STAT3 by corneal epithelial cells. The influence of IL-6, SIL-6R, or IL-6/SIL-6R on phosphorylation of STAT3 was examined by ELISA. IL-6 or IL-6/SIL-6R increased STAT3 phosphorylation as dose dependent, whereas SIL-6R alone did not induce the phosphorylation.

can be enhanced by the IL-6/SIL-6R complex. Cells that show balanced surface expression of IL-6R and gp130 also respond to IL-6, but this response is not altered by the IL-6/SIL-6R complex.[28–31] In this study, IL-6R protein was not detected on the surface of corneal fibroblasts, although RT-PCR detected mIL-6R at the mRNA level. In contrast, gp130 protein was expressed on the cell surface. These results indicate that corneal fibroblasts express fewer (or no) IL-6R molecules on the cell surface than gp130 molecules. Therefore, corneal fibroblasts responded to IL-6/SIL-6R and showed phosphorylation of STAT3 (the trans-signaling pathway). Our results were similar to those of another group.[17] On the other hand, expression of IL-6R and gp130 proteins on the surface of corneal epithelial cells was detected by flow cytometry. Therefore, corneal epithelial cells could respond to IL-6 alone by phosphorylation of STAT3 (the classic-signaling pathway), and this response was not altered by exposure of cells to IL-6/SIL-6R.

Recently, IL-6 has been suggested to play a role in corneal neovascularization. In the rat cornea micropocket assay, IL-6 was shown to induce corneal angiogenesis.[38] The present study indicated that stimulation by IL-6/SIL-6R leads to activation of STAT3 and the increased production of VEGF in corneal fibroblasts, whereas IL-6 alone did not have such an effect. One possible explanation for these results was that corneal fibroblasts express more gp130 molecules than mIL-6R molecules.

The first cells to participate in the inflammatory response related to wound healing are neutrophils, which infiltrate tissues and act as first line of defense against microorganisms. These neutrophils then undergo apoptosis and become an important source of SIL-6R. Recently, Chalaris et al.[39] demonstrated that shedding of SIL-6R from neutrophils was induced by apoptosis and that SIL-6R then promoted the trans-signaling pathway to regulate the attraction of monocytes involved in the clearance of apoptotic neutrophils. In this study, MCP-1 secretion was observed when corneal fibroblasts were treated with IL-6 alone, but the release of MCP-1 was significantly greater when cells were stimulated with IL-6/SIL-6R. Addition of SIL-6R alone also promoted a slight, but significant, increase of MCP-1 production, which suggests that IL-6 produced by corneal fibroblasts may bind to SIL-6R, resulting in activation of the IL-6/SIL-6R trans-signaling pathway. Thus, the SIL-6R/IL-6 complex may contribute to recruitment of monocytes into the

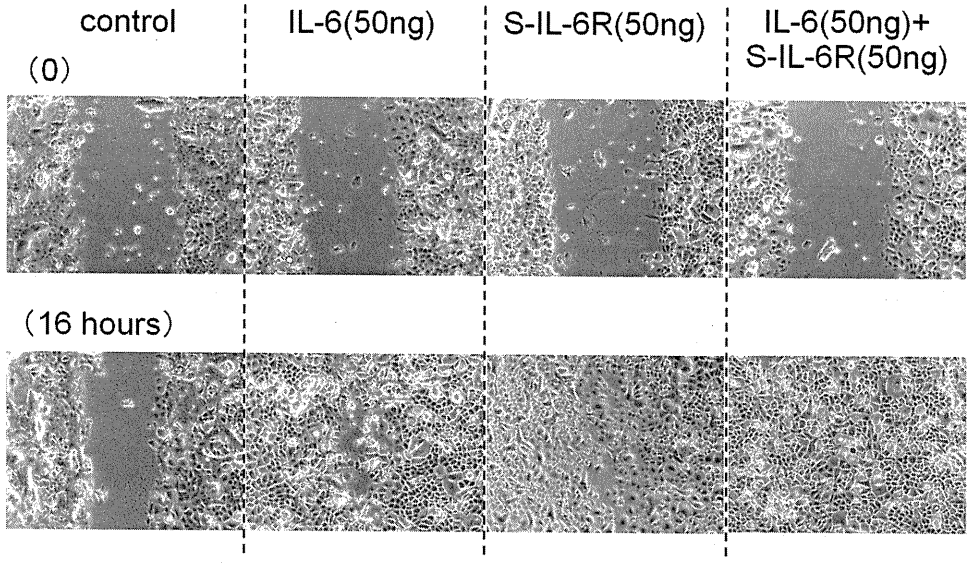

FIGURE 9. Corneal epithelial cell migration in the scratch assay. The scratch assay was done to assess in vitro migration of cultured corneal epithelial cells stimulated by IL-6, SIL-6R, or IL-6/SIL-6R. A uniform wound was made in each plate using a 200-μL pipette tip. The wound area was observed immediately and at 16 hours after creation. IL-6, SIL-6R, or IL-6/SIL-6R significantly induced cell migration compared with that by untreated cells.

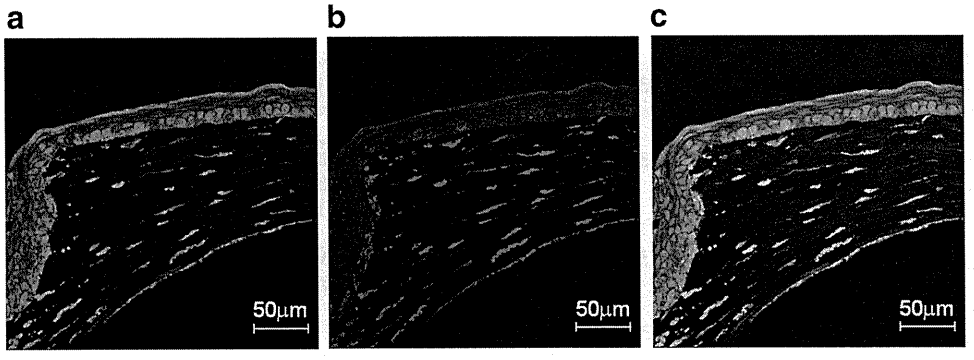

FIGURE 10. Expression of IL-6R and S100 A4 in mouse corneal wound healing model. Stromal injury was created by incision of the center of the cornea with a blade. Twenty-four hours after corneal injury, the expression of IL-6R and S100 A4 was observed by immunohistochemistry (**a**). Immunostaining for IL-6R (*green*) was observed in corneal fibroblasts at and nearby the site of injury. Immunostaining for IL-6R (*green*) was also recognized in basal cells of the epithelium near the site of injury and stratified epithelial cells at the site of injury (**b**). Immunostaining for S100 A4 (*red*), which was the marker of activated corneal fibroblasts, was observed in corneal fibroblasts at and nearby the site of injury (**c**). *Green* fluorescence from IL-6R and *red* fluorescence from S100 A4 identified activated corneal fibroblasts as expressing IL-6R (*yellow*) when the images were superimposed.

corneal stroma, resulting in the prevention of tissue damage from excessive inflammation by clearance of damaged/dead neutrophils,[40,41]

Previously, Nishida et al.[22–25] reported that IL-6 stimulates the migration of corneal epithelial cells both in vitro and in vivo. IL-6/STAT3 signaling also regulates human biliary epithelial cell migration and wound healing in vitro.[42] In the present study, IL-6 promoted the migration of corneal epithelial cells in the scratch assay, and IL-6/SIL-6R also induced migration of corneal epithelial cells in the same way as IL-6 alone. These results indicate that corneal epithelial cells show similar surface expression of IL-6R and gp130. Therefore, corneal epithelial cells responded to IL-6, and this response was not altered by addition of IL-6/SIL-6R. Surprisingly, however, SIL-6R itself promoted the migration of corneal epithelial cells. This raises the possibility that IL-6 produced by corneal epithelial cells bound to SIL-6R, resulting in the activation of these cells via the trans-signaling pathway. Furthermore, in our mouse corneal wound healing model, the expression of IL-6R and S100 A4 was recognized in corneal fibroblasts near the site of injury, revealing that activated fibroblasts express IL-6R. IL-6R expression was also recognized on basal cells near the site of injury. Therefore, IL-6 produced by corneal fibroblasts and IL-6R expression by activated fibroblasts and basal cells of the corneal epithelium may be important for corneal wound healing.

In conclusion, IL-1 derived from necrotic corneal epithelial cells induced the production of IL-6 by corneal fibroblasts. Activation of the IL-6 trans-signaling pathway induced the phosphorylation of STAT3, resulting in an increase of VEGF and MCP-1 production by corneal fibroblasts. Activation of the IL-6 classic-signaling pathway promoted the migration of corneal epithelial cells. IL-6R expression was also detected in activated fibroblasts and basal cells of the corneal epithelium during the processes of wound healing in vivo. These results emphasize the role of the IL-6 classic- and trans-signaling pathways in sterile inflammation of the cornea and corneal wound healing.

Acknowledgments

The authors thank Saori Ito and Ai Miyazaki for secretarial and technical assistance.

References

1. Matzinger P. The danger model: a renewed sense of self. *Science.* 2002;296:301–305.
2. Oppenheim JJ, Yang D. Alarmins: chemotactic activators of immune responses. *Curr Opin Immunol.* 2005;17:359–365.
3. Bianchi ME. DAMPs, PAMPs and alarmins: all we need to know about danger. *J Leukoc Biol.* 2007;81:1–5.
4. Chen CJ, Kono H, Golenbock D, et al. Identification of a key pathway required for the sterile inflammatory response triggered by dying cells. *Nat Med.* 2007;13:851–856.
5. Chen GY, Nuñez G. Sterile inflammation: sensing and reacting to damage. *Nat Rev Immunol.* 2010;10:826–837.
6. Wilson SE, Schultz GS, Chegini N, Weng J, He YG. Epidermal growth factor, transforming growth factor alpha, transforming growth factor beta, acidic fibroblast growth factor, basic fibroblast growth factor, and interleukin-1 proteins in the cornea. *Exp Eye Res.* 1994;59:63–71.
7. Wilson SE, He YG, Weng J, et al. Epithelial injury induces keratocyte apoptosis: hypothesized role for the interleukin-1 system in the modulation of corneal tissue organization and wound healing. *Exp Eye Res.* 1996;62:325–327.
8. Wilson SE, Liu JJ, Mohan RR. Stromal-epithelial interactions in the cornea. *Prog Retin Eye Res.* 1999;18:293–309.
9. Hong JW, Liu JJ, Lee JS, et al. Proinflammatory chemokine induction in keratocytes and inflammatory cell infiltration into the cornea. *Invest Ophthalmol Vis Sci.* 2001;42:2795–2803.
10. Stapleton WM, Chaurasia SS, Medeiros FW, et al. Topical interleukin-1 receptor antagonist inhibits inflammatory cell infiltration into the cornea. *Exp Eye Res.* 2008;86:753–757.
11. Wilson SE, Esposito A. Focus on molecules. Interleukin-1: a master regulator of the corneal response to injury. *Exp Eye Res.* 2009;89:124–125.
12. Weng J, Mohan RR, Li Q, Wilson SE. IL-1 upregulates keratinocyte growth factor and hepatocyte growth factor mRNA and protein production by cultured stromal fibroblast cells: interleukin-1 beta expression in the cornea. *Cornea.* 1997;16:465–471.
13. Yoon KC, Jeong IY, Park YG, Yang SY. Interleukin-6 and tumor necrosis factor-alpha levels in tears of patients with dry eye syndrome. *Cornea.* 2007;26:431–437.
14. Shoji J, Kawaguchi A, Gotoh A, Inada N, Sawa M. Concentration of soluble interleukin-6 receptors in tears of allergic conjunctival disease patients. *Jpn J Ophthalmol.* 2007;51:332–337.
15. Massingale ML, Li X, Vallabhajosyula M, et al. Analysis of inflammatory cytokines in the tears of dry eye patients. *Cornea.* 2009;28:1023–1027.
16. Lema I, Sobrino T, Durán JA, Brea D, Díez-Feijoo E. Subclinical keratoconus and inflammatory molecules from tears. *Br J Ophthalmol.* 2009;9:820–824.
17. Sugaya S, Sakimoto T, Shoji J, Sawa M. Regulation of soluble interleukin-6 (IL-6) receptor release from corneal epithelial cell and its role in the ocular surface. *Jpn J Ophthalmol.* 2011;55:277–282.
18. Simon D, Denniston AK, Tomlins PJ, et al. Soluble gp130, an antagonist of IL-6 transsignaling, is elevated in uveitis aqueous humor. *Invest Ophthalmol Vis Sci.* 2008;49:3988–3991.

19. Gallucci RM, Simeonova PP, Matheson JM, et al. Impaired cutaneous wound healing in interleukin-6-deficient and immunosuppressed mice. *FASEB J.* 2000;14:2525-2531.
20. Gallucci RM, Sugawara T, Yucesoy B, et al. Interleukin-6 treatment augments cutaneous wound healing in immunosuppressed mice. *J Interferon Cytokine Res.* 2001;21:603-609.
21. McFarland-Mancini MM, Funk HM, Paluch AM, et al. Differences in wound healing in mice with deficiency of IL-6 versus IL-6 receptor. *J Immunol.* 2010;184:7219-7228.
22. Nishida T, Nakamura M, Mishima H, Otori T, Hikida M. Interleukin 6 facilitates corneal epithelial wound closure in vivo. *Arch Ophthalmol.* 1992;110:1292-1294.
23. Nishida T, Nakamura M, Mishima H, Otori T. Interleukin 6 promotes epithelial migration by a fibronectin-dependent mechanism. *J Cell Physiol.* 1992;153:1-5.
24. Nakamura M, Nishida T. Differential effects of epidermal growth factor and interleukin 6 on corneal epithelial cells and vascular endothelial cells. *Cornea.* 1999;18:452-458.
25. Yamada N, Yanai R, Inui M, Nishida T. Sensitizing effect of substance P on corneal epithelial migration induced by IGF-1, fibronectin, or interleukin-6. *Invest Ophthalmol Vis Sci.* 2005;46:833-839.
26. Lam SP, Luk JM, Man K, et al. Activation of interleukin-6-induced glycoprotein 130/signal transducer and activator of transcription 3 pathway in mesenchymal stem cells enhances hepatic differentiation, proliferation, and liver regeneration. *Liver Transpl.* 2010;16:1195-1206.
27. Notara M, Shortt AJ, Galatowicz G, Calder V, Daniels JT. IL-6 and the human limbal stem cell niche: a mediator of epithelial-stromal interaction. *Stem Cell Res.* 2010;5:188-200.
28. Peters M, Müller AM, Rose-John S. Interleukin-6 and soluble interleukin-6 receptor: direct stimulation of gp130 and hematopoiesis. *Blood.* 1998;92:3495-3504.
29. Kamimura D, Ishihara K, Hirano T. IL-6 signal transduction and its physiological roles: the signal orchestration model. *Rev Physiol Biochem Pharmacol.* 2003;149:1-38.
30. Rabe B, Chalaris A, May U, et al. Transgenic blockade of interleukin 6 transsignaling abrogates inflammation. *Blood.* 2008;111:1021-1028.
31. Drucker C, Gewiese J, Malchow S, Scheller J, Rose-John S. Impact of interleukin-6 classic- and trans-signaling on liver damage and regeneration. *J Autoimmun.* 2010;34:29-37.
32. Jones SA, Horiuchi S, Topley N, Yamamoto N, Fuller GM. The soluble interleukin 6 receptor: mechanisms of production and implications in disease. *FASEB J.* 2001;15:43-58.
33. Matthews V, Schuster B, Schütze S, et al. Cellular cholesterol depletion triggers shedding of the human interleukin-6 receptor by ADAM10 and ADAM17 (TACE). *J Biol Chem.* 2003;278:38829-38839.
34. Scaffidi P, Misteli T, Bianchi ME. Release of chromatin protein HMGB1 by necrotic cells triggers inflammation. *Nature.* 2002;418:191-195.
35. Ryan DG, Taliana L, Sun L, et al. Involvement of S100A4 in stromal fibroblasts of the regenerating cornea. *Invest Ophthalmol Vis Sci.* 2003;44:4255-4262.
36. Sotozono C, He J, Matsumoto Y, Kita M, Imanishi J, Kinoshita S. Cytokine expression in the alkali-burned cornea. *Curr Eye Res.* 1997;16:670-676.
37. Biswas PS, Banerjee K, Kim B, Rouse BT. Mice transgenic for IL-1 receptor antagonist protein are resistant to herpetic stromal keratitis: possible role for IL-1 in herpetic stromal keratitis pathogenesis. *J Immunol.* 2004;172:3736-3744.
38. Ebrahem Q, Minamoto A, Hoppe G, Anand-Apte B, Sears JE. Triamcinolone acetonide inhibits IL-6- and VEGF-induced angiogenesis downstream of the IL-6 and VEGF receptors. *Invest Ophthalmol Vis Sci.* 2006;47:4935-4941.
39. Chalaris A, Rabe B, Paliga K, et al. Apoptosis is a natural stimulus of IL6R shedding and contributes to the proinflammatory trans-signaling function of neutrophils. *Blood.* 2007;110:1748-1755.
40. Romano M, Sironi M, Toniatti C, et al. Role of IL-6 and its soluble receptor in induction of chemokines and leukocyte recruitment. *Immunity.* 1997;6:315-325.
41. Hurst SM, Wilkinson TS, McLoughlin RM, et al. IL-6 and its soluble receptor orchestrate a temporal switch in the pattern of leukocyte recruitment seen during acute inflammation. *Immunity.* 2001;14:705-714.
42. Jiang GX, Zhong XY, Cui YF, et al. IL-6/STAT3/TFF3 signaling regulates human biliary epithelial cell migration and wound healing in vitro. *Mol Biol Rep.* 2010;37:3813-3818.

Noninvasive Observations of Peripheral Angle in Eyes After Penetrating Keratoplasty Using Anterior Segment Fourier-Domain Optical Coherence Tomography

Reina Fukuda, MD, Tomohiko Usui, MD, Atsuo Tomidokoro, MD, Koichi Mishima, MD, Naomi Matagi, MD, Takashi Miyai, MD, Shiro Amano, MD, and Makoto Araie, MD

Purpose: To examine iridotrabecular contact (ITC) as a peripheral anterior synechia (PAS) of patients who underwent penetrating keratoplasty (PKP) using anterior segment Fourier-domain optical coherence tomography (OCT).

Methods: Retrospective, observational case series. ITC, ITC index, and ITC area of 60 eyes of 52 patients who underwent PKP at the Department of Ophthalmology in the University of Tokyo Hospital (mean follow-up time 102.8 ± 116.1 months postoperation) were calculated using the angle analysis mode of a commercially available anterior segment Fourier-domain OCT system (CASIA; TOMEY, Nagoya, Japan). We analyzed the occurrence of ITC, ITC index, and ITC area with preoperative diagnosis, lens status, operation method, operation frequency, graft size, and intraocular pressure elevation.

Results: ITC was observed in 28 (46.7%) of 60 eyes. Average ITC index was 14.0%, and average ITC area was 5.97 mm^2. ITC was significantly associated with eyes with bullous keratopathy, infectious keratitis, pseudophakia, PKP with cataract operation, several PKP operations, and large graft size.

Conclusions: Anterior segment Fourier-domain OCT is a useful and innovative tool that enables us to observe the anterior chamber angle and examine ITC as PAS of eyes with corneal opacity, even after PKP.

Key Words: penetrating keratoplasty, iridotrabecular contact, peripheral anterior synechia, anterior segment optical coherence tomography

(*Cornea* 2012;31:259–263)

Penetrating keratoplasty (PKP) is still a gold standard surgery for replacing opaque cornea. However, many complications may occur after PKP, including peripheral anterior synechia (PAS). Because PAS is recognized as one of the risk factors for graft rejection[1] and may occasionally cause intraocular pressure (IOP) elevation,[2] it is important to evaluate anterior chamber angle in eyes after PKP. Because eyes after PKP tend to have peripheral corneal opacity, it is often difficult to evaluate anterior chamber angle with a gonioscope and a slit lamp. Ultrasound biomicroscopy (UBM) is a useful tool for the observation of angle structures of eyes with hazy corneas.[3] However, UBM necessitates direct contact with the eyes, which can be invasive, especially in eyes soon after the operation.

Optical coherence tomography (OCT) is a noncontact imaging technology that allows cross-sectional imaging of biologic systems.[4] Compared with traditional time-domain OCT systems, newly introduced Fourier-domain OCT systems enable high-speed, high-resolution, and 3-dimensional imaging.[5,6] Fourier-domain OCT systems, which are based on spectral interferometry, are classified into spectral-domain OCT and swept source (SS)-OCT. In the spectral-domain OCT, the spectral interferogram is snapped by a detector array with a wideband light source, whereas SS-OCT uses frequency sweeping or a tunable laser to produce the spectral interferogram.[7,8] For the assessment of anterior ocular segment structures, an anterior segment SS-OCT system (AS-SS-OCT, CASIA SS-1000; TOMEY, Nagoya, Japan) has been recently developed. The AS-SS-OCT system with a light source with wavelength of 1310 nm allows higher speed of data acquisition, greater imaging depth, and wider observable range. This device enabled us to observe anterior chamber angles of 360 degrees even in eyes with opaque corneas in a noninvasive manner. The purpose of this study was to evaluate the prevalence and amount of iridotrabecular contact (ITC), which involves both adhesive and appositional contact of the peripheral iris with the trabecular meshwork,[9,10] in eyes after PKP using AS-SS-OCT.

MATERIALS AND METHODS

The study was approved by the Institutional Review Board of the University of Tokyo School of Medicine (Tokyo, Japan). Written informed consent was obtained from all patients. The retrospective, observational, cross-sectional study population constituted 60 eyes of 52 patients (29 men and 23 women) who underwent PKP in the past and had medical examination between July 2009 and January 2010 at the outpatient clinic of the Department of Ophthalmology, Graduate School of Medicine, University of Tokyo. All patients underwent slit-lamp examination, IOP measurements, and anterior segment measurements by AS-SS-OCT.

Received for publication November 24, 2010; revision received May 19, 2011; accepted May 30, 2011.
From the Department of Ophthalmology, University of Tokyo School of Medicine, Tokyo, Japan.
The authors state that they have no proprietary interest in the products named in this article.
Reprints: Tomohiko Usui, 7-3-1 Hongo, Bunkyo-ku, Tokyo 113-8655, Japan (e-mail: tomohiko-tky@umin.ac.jp).

IOP was measured with Goldmann applanation tonometry in 52 eyes or with pneumatic tonometry (Model 30 classic; Medtronic Solar, Jacksonville, FL) in 8 eyes in which applanation tonometry was inaccurate because of the deformed cornea. The anterior ocular segment was imaged with the biangle radial scan protocol (angle analysis mode) of AS-SS-OCT. This protocol consists of 128 radial B-scans of 16 mm long centered on the corneal center, and each of the B-scans includes 512 A-scans. The measurement time was 2.3 seconds per each eye. During the examination, patients were encouraged to open their eyes as wide as possible. If necessary, the examiner used fingers to open the patients' eyes wide enough to make the best possible observations without pressing the eye balls. When motion or blinking of the eyes bothered accurate examination, the practice was repeated up to 3 times, and the best image was selected for the analysis.

The concept of ITC includes both adhesive and appositional contact of the peripheral iris with the trabecular meshwork or corneal endothelium.[9,10] The presence of and the area of ITC in the 360-degree angle of the peripheral anterior chamber were determined with a software newly developed by the manufacturer. With the software, the scleral spur (SS) and the peripheral end point of the iris (EP) in both sides were plotted by an ophthalmologist (R.F.) in at least 80 of the acquired 128 B-scan images, and then SS and EP were automatically extrapolated in the other images (Fig. 1). The automatically determined positions of SS and EP were confirmed in all B-scan images by the ophthalmologist and if necessary corrected manually. When EP was located more proximally than SS in 3 consecutive B-scan images, it was supposed that there was ITC at that position. In many of the eyes, the analysis could not be performed in some areas out of 360 degrees because of the absence of images by the under or upper eye lid coverage, and the area was called an "invisible range." The parameters automatically calculated were ITC area, the sum of the areas of ITC in an eye; ITC index, the percent of degrees that had ITC out of the visible range; and the invisible range in degrees. The anterior chamber depth, as the distance between the posterior corneal surface and the anterior lens surface, was also determined manually in a horizontal B-scan image.

In the present study, we evaluated the prevalence of ITC, ITC index, and ITC area and assessed the association of ITC with preoperative diagnosis. Second, because infectious cases often involve PAS preoperatively, they were excluded from the assessment of ITC with lens status, operation method, operation frequency, graft size, and IOP elevation. Statistical analysis was performed using the Mann–Whitney U test, Kruskal–Wallis H test, and 2×2 and Yates $m \times n$ χ^2 test.

RESULTS

Of the 60 eyes of 52 patients who underwent PKP at the Department of Ophthalmology, University of Tokyo Hospital, from 1973 to January 2010, age ranged from 19 to 88 years (mean age, 63.8 ± 14.3 years). Preoperative diagnoses were bullous keratopathy in 24 eyes (40%), infectious keratitis in 19 eyes (31.7%), corneal dystrophies in 8 eyes (13.3%), and keratoconus in 9 eyes (15%). The causes of bullous keratopathy were laser iridectomy in 7 eyes, trabeculectomy in 6 eyes, trauma in 5 eyes, cataract surgery in 3 eyes, and unknown causes in 3 eyes. Mean postoperative period was 101.2 months and ranged from 1 month to 444 months. This includes patients who underwent several PKP operations, ranging from 1 to 6 times, counting the postoperative period from the latest operation.

ITC was observed in 28 (46.7%) of the 60 eyes. Among the 60 eyes examined, average invisible area was 89.1 ± 74.5 mm^2, ITC area averaged was 5.97 mm^2 [95% confidence interval (CI), 3.05–8.89 mm^2; range, 0 mm^2–51.68 mm^2], ITC

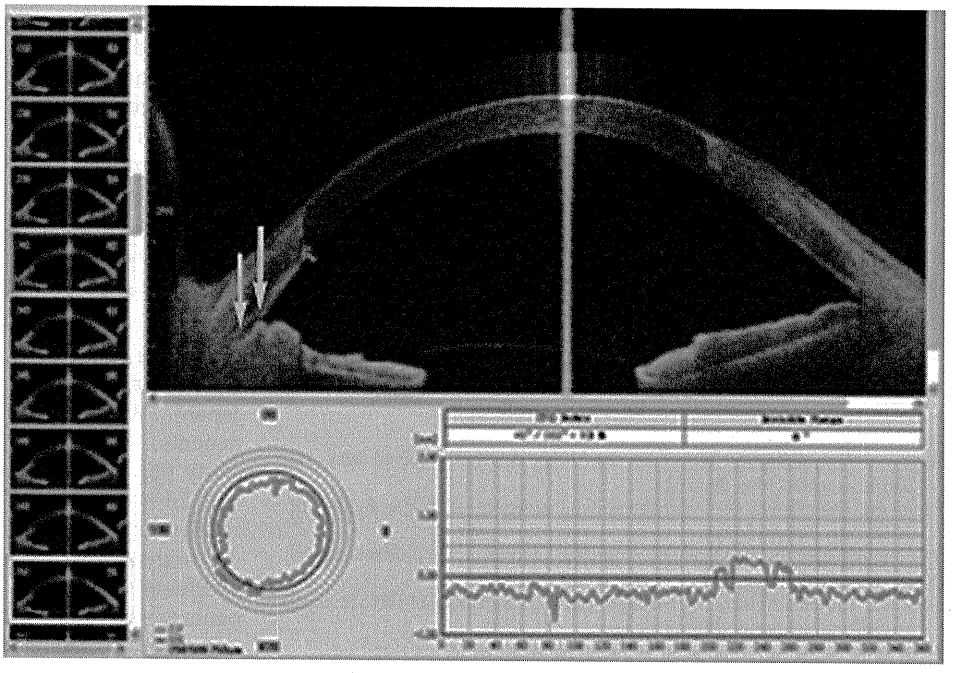

FIGURE 1. Example of anterior segment Fourier-domain OCT images in eyes after PKP. Arrows indicate SS (right) and EP (left).

index was 14.03% (95% CI, 8.73%–19.33%; range, 0%–92.0%), and anterior chamber depth was 3.04 mm (95% CI, 2.88–3.20 mm; range, 1.69 mm–4.12 mm).

The prevalence of ITC, ITC area, and ITC index stratified by the preoperative diagnoses is summarized in Table 1. The prevalence of ITC was the highest in eyes having bullous keratopathy, whereas the ITC area and ITC index were the largest in eyes having bullous keratopathy or infectious keratitis preoperatively. No ITC was found in eyes with keratoconus (Figs. 2, 3).

Table 2 summarizes the prevalence of ITC, ITC area, and ITC index divided by the present lens status and other conditions on PKP surgery, including combined cataract surgery, history of PKP, and graft size. As shown in Table 2, significant factors associated with the higher prevalence of ITC and greater values of ITC area and ITC index were pseudophakic eyes, combined procedure of open-sky cataract extraction, history of PKP, and graft size of 7.75 mm or larger.

In 9 (22.0%) of the 41 eyes, IOP was higher than 21 mm Hg. Prevalence of ITC was not significantly different between the eyes with IOP $\geq$ 21 mm Hg and the eyes with IOP $<$ 21 mm Hg [7 of 9 (77.8%) vs. 14 of 32 (43.8%); $P = 0.13$; 2×2 χ^2 test]. These results are summarized in Table 3.

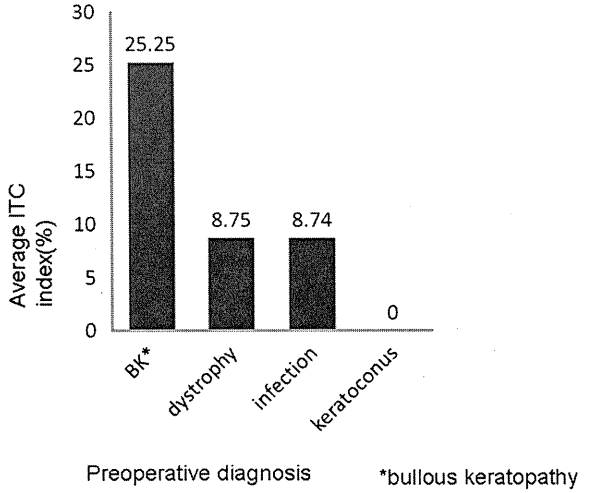

FIGURE 2. Prevalence of average ITC index (%) found in (BK) various operation indications for PKP. Bullous keratopathy shows the highest ITC index, whereas keratoconus shows the least.

DISCUSSION

The current study demonstrates that AS-SS-OCT enables us to observe anterior chamber angle and to quantitatively evaluate ITC even in eyes after PKP, in most of which the angle was hardly observed using a gonioscope because of the peripheral or total corneal opacity. The clinical concept of ITC involves both PAS and appositional closure,[9,10] roles of which should be different in eyes with primary angle closure or suspected angle closure. ITC is often evaluated in patients with a shallow peripheral anterior chamber because of the risk of trabecular damage, elevated IOP, and acute angle closure. Appositional closure is reversible and nonpermanent, whereas PAS refers to a condition in which iris adheres to the angle anteriorly, possibly as a result of prolonged appositional closure.[11,12] However, these 2 closure mechanisms are often difficult to differentiate with untouched evaluations of the anterior chamber with UBM or anterior segment OCT because of the lack of indentation technique. In the current study on eyes after PKP, because the height of the most ITC was apparently higher than the Schwalbe line and the border lines of the ITC were very irregular, the observed height and range of ITC should be nearly equal to those of PAS. Evaluation of ITC in terms of PAS is also essential in other ocular conditions, such as uveitis, iris neovascularization, and postintraocular surgery, because not only may it reflect severity and duration of inflammation or disease activity but also it may relate to the magnitude of IOP elevation preceding visual field defects.[13,14]

Despite the importance of the evaluation of peripheral anterior chamber angle in eyes after PKP, as mentioned in the Introduction, our knowledge of it is still limited probably because of difficulties in the accurate assessment of angle structures through opaque corneas. Dada et al[15] found PAS in 30 (97%) of 31 eyes with IOP elevation after PKP using UBM with 12 clockwise sections. On the other hand, considerably lower prevalence rates of PAS were reported, such as 19 (8%) of 229 eyes[16] or 52 (19%) of 269 eyes[17] after PKP with or without IOP elevation. In those reports, the presence of PAS should be determined according to slit-lamp findings alone, although the methods were not described specifically. In the current study using AS-SS-OCT, the observation covered the whole 360-degree angle with 128 sections except for the invisible area mainly because of the eyelid coverage. Our results showed a lower prevalence of ITC than the result from the UBM study because their study group included post-PKP glaucoma patients, who underwent a therapeutic keratoplasty for a perforated corneal ulcer or an optical keratoplasty for corneoiridic scars. To avoid the risk of infection and leakage, use of UBM would be undesirable especially soon after PKP. The presence of ITC observed with AS-SS-OCT was more frequent than that observed with the slit lamp, probably

TABLE 1. Association of ITC, ITC Index, and ITC Area With Preoperative Diagnosis

	Prevalence of ITC, n (%)	ITC Area, Mean ± SD (Range), mm^2	ITC Index, Mean ± SD (Range), %
Bullous keratopathy	17/24 (70.1)	9.79 ± 14.30 (4.07–15.51)	25.25 ± 25.77 (14.95–35.55)
Infectious keratitis	7/19 (36.8)	19.76 ± 11.30 (14.68–24.84)	8.76 ± 16.08 (1.53–15.99)
Corneal dystrophies	4/8 (50)	1.94 ± 2.99 (0–4.01)	8.75 ± 9.66 (2.06–15.44)
Keratoconus	0/9 (0)	0	0
P	0.0025	0.0058	0.0008
Total	46.7	5.97 ± 11.55	14.03 ± 20.96

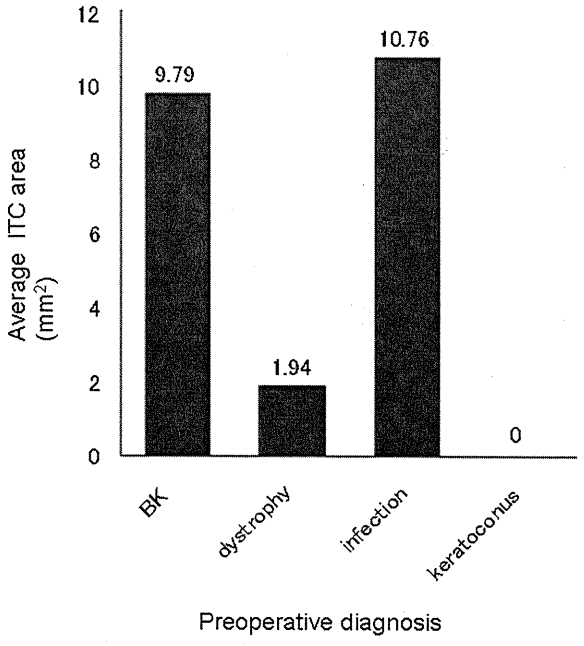

FIGURE 3. Prevalence of average ITC area (in square millimeters) found in various operation indications for PKP. Bullous keratopathy and infection shows greater average ITC area among the others.

because of the inability of the slit lamp to examine precisely through opaque corneas.

In the current study, corneal diseases before PKP operation had a major impact on the prevalence of ITC. There were statistically significant differences in ITC, ITC area, and ITC index among the 4 groups of pre-PKP corneal diseases, including keratoconus, bullous keratopathy, corneal dystrophy, and infectious keratitis. Apparently, ITC was not found in post-PKP eyes after keratoconus, whereas eyes showed higher prevalence of ITC after bullous keratopathy or infectious keratitis. Possible explanations for the absence of ITC in keratoconus eyes are that the eyes had sufficient anterior chamber depth (averaged 3.79 ± 0.58 mm in the central anterior chamber) for avoiding the ITC formation and that the graft size in PKP surgery in keratoconus eyes was generally small, resulting in a lesser influence on the peripheral anterior chamber and smaller antigenic load. Keratoconus is a non-inflammatory ectatic corneal disease, which has traditionally reported excellent success rates among the other groups of patients undergoing PKP.[18,19] Average ITC area was the largest in eyes having infectious keratitis before PKP probably because large amount of PAS existed before PKP in such eyes due to severe infectious reaction. On the other hand, eyes with keratoconus or corneal dystrophy generally have no ITC or PAS before PKP, also resulting in no or low prevalence of ITC after PKP.

TABLE 2. Association of ITC, ITC Index, and ITC Area With Each Parameter

	Prevalence of ITC, n (%)	Average ITC Index, %	Average ITC Area, mm²
Phakia	3/14 (21.4)	7.9	2.1
Pseudophakia/aphakia	18/27 (66.7)	21.7	7.5
P	0.009*	0.014†	0.012†
PKP+ECCE	10/13 (76.9)	29.0	11.3
PKP	11/28 (39.2)	10.7	2.75
P	0.043*	0.021†	0.022†
PKP once	11/30 (36.7)	12.3	3.9
PKP twice or more	10/11 (90.9)	27.8	9.7
P	0.004*	0.009†	0.002†
Graft size <7.75 mm	4/13 (30.8)	16.5	7.6
Graftsize ≥7.75 mm	16/22 (72.7)	20.1	5.8
P	0.032*	0.041†	0.040†

*χ^2 test.
†Mann-Whitney *U* test.
ECCE, extracapsular cataract extraction.

TABLE 3. Association of ITC, ITC Index, and ITC Area With IOP

	Prevalence of ITC, n (%)	Average ITC Index, %	Average ITC Area, mm²
IOP ≥ 21 mm Hg	7/9 (77.8)	18.8	5.2
IOP < 21 mm Hg	14/32 (43.8)	15.8	5.5
P	0.13*	0.09†	0.11†

*χ^2 test.
†Mann-Whitney *U* test.

This study evaluated the prevalence of ITC, ITC index, and ITC area with lens status, operation method, operation frequency, graft size, and IOP elevation among post-PKP eyes. This analysis did not include infectious cases, which vary in postoperative outcomes, depending on sizes of ulcer and existence of perforation. Incidence of reinfection, anterior synechia, and glaucoma were reported to be more frequent with large grafts required for large ulcers.[20]

Prevalence and area of ITC were greater in pseudophakic or aphakic eyes compared with phakic eyes. Patients with phakic eyes tended to be young, and most of them had keratoconus as a pre-PKP disease, probably resulting in a smaller amount of ITC after PKP. In other words, all of the 9 keratoconus eyes were phakic eyes in this study; thus further assessment of lens status with ITC among keratoconus eyes would be worthwhile. Combined surgeries of cataract extraction with or without intraocular lens implantation in addition to PKP were also associated with great amounts of ITC compared with PKP operation alone. Additional manipulations of cataract extraction and intraocular lens implantation often results in eyeball collapse, leading to the formation of PAS postoperatively. Similarly, ITC was observed more in eyes with several PKP operations, probably because of frequent eyeball collapse under repeated open-sky maneuvers. In a previous study, the rates of PAS were substantially higher in patients who had undergone repeated PKP surgeries.[21]

Large graft size was also associated with a higher amount of ITC. In eyes with larger grafts, the PKP procedure required maneuvers close to the corneal limbus and the graft–host junction was located more peripherally after the surgery, both of which were likely to generate PAS. Thus, lens

condition, combined surgery, several PKP operations, and large graft size were associated with a greater amount of ITC in patients of the present study. However, the distributions of corneal diseases before PKP were not equal among groups of the above conditions, for example, bullous keratopathy was more frequent in eyes with pseudophakia, history of combined surgeries or several PKP operations, and/or large graft size in PKP. Because of the limited number of the studied patients, it was difficult to statistically exclude the influence of the unequal distribution of pre-PKP diseases from those comparisons, and this deserves further investigations including more patients in a prospective study design.

Glaucoma or elevation of IOP is one of the most serious complications after PKP.[22] Its incidence has been reported to range from 10% to 53%.[21–29] In the previous studies, risk factors for the escalation of glaucoma therapies were pre-PKP ocular diseases, such as infection, trauma, and bullous keratopathy; older age; preexisting glaucoma; presence of pseudophakia or aphakia; smaller (less than 7.0 mm) recipient trephination; cataract and/or anterior vitrectomy combined surgery; and graft thinning.[21,22,26,29] Mechanisms of IOP elevation are considered to comprise synechial angle closure, the use of topical steroids, trabeculitis, and blocked drainage tube.[22,23] Simple statistical analysis in our study showed that the amount of post-PKP ITC was not associated with increased IOP. Among the patients with elevated IOP, average ITC index was only 18.8%, a relatively small percentage in the blockage of trabecular meshwork because mean PAS extent in primary angle closure eyes with IOP elevation was reportedly 101.6 ± 16.1 degrees.[30] However, when we included infectious cases in this statistical analysis, IOP elevation was significantly associated with the prevalence of ITC ($P = 0.01$, χ^2 test) and the amount of ITC index and ITC area ($P = 0.002$ and $P = 0.003$, respectively, Mann–Whitney U test). Besides, infectious cases alone were not significantly related with IOP elevation compared with noninfectious cases ($P = 0.2$, χ^2 test). Thus, from the present results, ITC or PAS can be one of the possible risk factors for IOP elevation after PKP, although it may not be a main causal factor.

In conclusion, using high-resolution AS-SS-OCT, anterior chamber angles of eyes after PKP could be noninvasively visualized even in eyes with opaque corneas, and ITC could be quantitatively evaluated. Associations of the presence and the amount of ITC with preoperative corneal diseases and some operation-related factors were statistically significant. The information on peripheral anterior chamber angles in eyes after PKP should be clinically useful to follow-up the patients and, when necessary, to decide the incision site for glaucoma surgeries, including trabeculectomy, trabeculotomy, and shunt tube implantation.

REFERENCES

1. Yamagami S, Suzuki Y, Tsuru T. Risk factors for graft failure in penetrating keratoplasty. *Acta Ophthalmol Scand.* 1996;74:584–588.
2. Memarzadeh F, Li Y, Francis BA, et al. Optical coherence tomography of the anterior segment in secondary glaucoma with corneal opacity after penetrating keratoplasty. *Br J Ophthalmol.* 2007;91:189–192.
3. Yoo C, Oh JH, Kim YY, et al. Peripheral anterior synechiae and ultrasound biomicroscopic parameters in angle-closure glaucoma suspects. *Korean J Ophthalmol.* 2007;21:106–110.
4. Huang D, Swanson EA, Lin CP, et al. Optical coherence tomography. *Science.* 1991;254:1178–1181.
5. Wylegała E, Teper S, Nowińska AK, et al. Anterior segment imaging: Fourier-domain optical coherence tomography versus time-domain optical coherence tomography. *J Cataract Refract Surg.* 2009;35:1410–1414.
6. Asrani S, Sarunic M, Santiago C, et al. Detailed visualization of the anterior segment using Fourier-domain optical coherence tomography. *Arch Ophthalmol.* 2008;126:765–771.
7. Liu B, Azimi E, Brezinski ME. Improvement in dynamic range limitation of swept source optical coherence tomography by true logarithmic amplification. *J Opt Soc Am A Opt Image Sci Vis.* 2010;27:404–414.
8. Nakagawa T. Anterior segment OCT (Visante OCT). *Ganka Shujyutsu.* 2008;21:213–215.
9. Barkana Y, Dorairaj SK, Gerber Y, et al. Agreement between gonioscopy and ultrasound biomicroscopy in detecting iridotrabecular apposition. *Arch Ophthalmol.* 2007;125:1331–1335.
10. Liu L. Anatomical changes of the anterior chamber angle with anterior-segment optical coherence tomography. *Arch Ophthalmol.* 2008;126:1682–1686.
11. Dorairaj SK, Tello C, Liebmann JM, et al. Narrow angles and angle closure: anatomic reasons for earlier closure of the superior portion of the iridocorneal angle. *Arch Ophthalmol.* 2007;125:734–739.
12. Kunimatsu S, Tomidokoro A, Mishima K, et al. Prevalence of appositional angle closure determined by ultrasonic biomicroscopy in eyes with shallow anterior chambers. *Ophthalmology.* 2005;112:407–412.
13. Kronfeld PC. Delayed restoration of the anterior chamber. The eighth Proctor lecture. *Am J Ophthalmol.* 1954;38:453–465.
14. Choi JS, Kim YY. Relationship between the extent of peripheral anterior synechiae and the severity of visual field defects in primary angle-closure glaucoma. *Korean J Ophthalmol.* 2004;18:100–105.
15. Dada T, Aggarwal A, Vanathi M, et al. Ultrasound biomicroscopy in opaque grafts with post-penetrating keratoplasty glaucoma. *Cornea.* 2008;27:402–405.
16. Simmons RB, Stern RA, Teekhasaenee C, et al. Elevated intraocular pressure following penetrating keratoplasty. *Trans Am Ophthalmol Soc.* 1989;87:79–93.
17. Inoue K, Amano S, Oshika T, et al. Risk factors for corneal graft failure and rejection in penetrating keratoplasty. *Acta Ophthalmol Scand.* 2001;79:251–255.
18. Fukuoka S, Honda N, Ono K, et al. Extended long-term results of penetrating keratoplasty for keratoconus. *Cornea.* 2010;29:528–530.
19. Sharif KW, Casey TA. Penetrating keratoplasty for keratoconus: complications and long-term success. *Br J Ophthalmol.* 1991;75:142–146.
20. Sukhija J, Jain AK. Outcome of therapeutic penetrating keratoplasty in infectious keratitis. *Ophthalmic Surg Lasers Imaging.* 2005;36:303–307.
21. Weisbrod DJ, Sit M, Naor J, et al. Outcomes of repeat penetrating keratoplasty and risk factors for graft failure. *Cornea.* 2003:22:429–434.
22. Franca ET, Arcieri ES, Arcieri RS, et al. A study of glaucoma after penetrating keratoplasty. *Cornea.* 2002;21:284–288.
23. Ayyala RS. Penetrating keratoplasty and glaucoma. *Surv Ophthalmol.* 2000;45:91–105.
24. Ikeda K, Fukuoka S, Usui T, et al. Trabeculectomy for glaucoma after penetrating keratoplasty. *Atarashii Ganka.* 2008;25:219–221.
25. Sugioka K, Fukuda M, Hibino T, et al. Retrospective study of secondary glaucoma after penetrating keratoplasty at Kinki university hospital. *Atarashii Ganka.* 2001;18:948–951.
26. Erdurmus M, Cohen EJ, Yildiz EH, et al. Steroid-induced intraocular pressure elevation or glaucoma after penetrating keratoplasty in patients with keratoconus or fuchs dystrophy. *Cornea.* 2009;28:759–764.
27. Chua J, Mehta JS, Tan DT. Use of anterior segment optical coherence tomography to assess secondary glaucoma after penetrating keratoplasty. *Cornea.* 2009;28:243–245.
28. Al-Mohaimeed M, Al-Shahwan S, Al-Torbak A, et al. Escalation of glaucoma therapy after penetrating keratoplasty. *Ophthalmology.* 2007;114:2281–2286.
29. Karadag O, Kugu S, Erdogan G, et al. Incidence of and risk factors for increased intraocular pressure after penetrating keratoplasty. *Cornea.* 2010;29:278–282.
30. Lee JY, Kim YY, Jung HR. Distribution and characteristics of peripheral anterior synechiae in primary angle-closure glaucoma. *Korean J Ophthalmol.* 2006;20:104–108.

OPEN ACCESS Freely available online

PLoS one

Prostaglandin E Receptor Subtype EP3 Expression in Human Conjunctival Epithelium and Its Changes in Various Ocular Surface Disorders

Mayumi Ueta[1,2]*, Chie Sotozono[1], Norihiko Yokoi[1], Tsutomu Inatomi[1], Shigeru Kinoshita[1]

1 Department of Ophthalmology, Kyoto Prefectural University of Medicine, Kyoto, Japan, **2** Research Center for Inflammation and Regenerative Medicine, Faculty of Life and Medical Sciences, Doshisha University, Kyoto, Japan

Abstract

Background: In our earlier genome-wide association study on Stevens-Johnson Syndrome (SJS) and its severe variant, toxic epidermal necrolysis (TEN), we found that in Japanese patients with these severe ocular surface complications there was an association with prostaglandin E receptor 3 (EP3) gene (*PTGER3*) polymorphisms. We also reported that EP3 is dominantly expressed in the ocular surface-, especially the conjunctival epithelium, and suggested that EP3 in the conjunctival epithelium may down-regulate ocular surface inflammation. In the current study we investigated the expression of EP3 protein in the conjunctiva of patients with various ocular surface diseases such as SJS/TEN, chemical eye burns, Mooren's ulcers, and ocular cicatricial pemphigoid (OCP).

Methodology/Principal Findings: Conjunctival tissues were obtained from patients undergoing surgical reconstruction of the ocular surface due to SJS/TEN, chemical eye burns, and OCP, and from patients with Mooren's ulcers treated by resection of the inflammatory conjunctiva. The controls were nearly normal human conjunctival tissues acquired at surgery for conjunctivochalasis. We performed immunohistological analysis of the EP3 protein and evaluated the immunohistological staining of EP3 protein in the conjunctival epithelium of patients with ocular surface diseases. EP3 was expressed in the conjunctival epithelium of patients with chemical eye burns and Mooren's ulcer and in normal human conjunctival epithelium. However, it was markedly down-regulated in the conjunctival epithelium of SJS/TEN and OCP patients.

Conclusions: We posit an association between the down-regulation of EP3 in conjunctival epithelium and the pathogenesis and pathology of SJS/TEN and OCP, and suggest a common mechanism(s) in the pathology of these diseases. The examination of EP3 protein expression in conjunctival epithelium may aid in the differential diagnosis of various ocular surface diseases.

Citation: Ueta M, Sotozono C, Yokoi N, Inatomi T, Kinoshita S (2011) Prostaglandin E Receptor Subtype EP3 Expression in Human Conjunctival Epithelium and Its Changes in Various Ocular Surface Disorders. PLoS ONE 6(9): e25209. doi:10.1371/journal.pone.0025209

Editor: Naj Sharif, Alcon Research, Ltd., United States of America

Received June 14, 2011; **Accepted** August 29, 2011; **Published** September 22, 2011

Funding: This work was supported in part by grants-in-aid for scientific research from the Japanese Ministry of Health, Labour and Welfare, the Japanese Ministry of Education, Culture, Sports, Science and Technology, CREST from JST, a research grant from the Kyoto Foundation for the Promotion of Medical Science, and the Intramural Research Fund of Kyoto Prefectural University of Medicine. The funders had no role in study design, data collection and analysis, decision to publish, or preparation of the manuscript.

Competing Interests: The authors have declared that no competing interests exist.

* E-mail: mueta@koto.kpu-m.ac.jp

Introduction

Prostanoids are comprised of prostaglandins (PGs) and thromboxanes (TXs). They are lipid mediators that form in response to various stimuli and include PGD_2, PGE_2, $PGF_{2\alpha}$, PGI_2, and TXA_2. They are released extracellularly immediately after their synthesis and they act by binding to a G-protein-coupled rhodopsin-type receptor on the surface of target cells. There are 8 types of prostanoid receptors that are conserved in mammals from mouse to human: the PGD receptor (DP), 4 subtypes of the PGE receptor (EP1, EP2, EP3, and EP4), the PGF receptor (FP), the PGI receptor (IP), and the TXA receptor (TP) [1].

Stevens-Johnson syndrome (SJS) and its severe variant, toxic epidermal necrolysis (TEN) are acute inflammatory vesiculobullous reactions of the skin and mucosa including the ocular surface [2]. In our earlier genome-wide association study in Japanese SJS/TEN patients with severe ocular surface complications we found associations with 6 single nucleotide polymorphisms (SNPs) in the prostaglandin E receptor 3 (EP3) gene (*PTGER3*) and we documented that compared with the controls, EP3 expression was markedly reduced in the conjunctival epithelium of SJS/TEN patients with severe ocular complications [3]. Others reported that the PGE_2-EP3 signaling pathway negatively regulates allergic reactions in a murine allergic asthma model [4] and that it inhibits keratinocyte activation and exerts anti-inflammatory actions in mouse contact hypersensitivity [5]. We also showed that EP3 is dominantly expressed in the ocular surface-, especially the conjunctival epithelium, and that PGE_2 acts as a ligand for EP3 in the conjunctival epithelium and down-regulates the progression of murine experimental allergic conjunctivitis [6]. In addition, we reported that an EP3 agonist suppressed the production of CCL5, CXCL10, CXCL11, and IL-6 in response to polyI:C stimulation

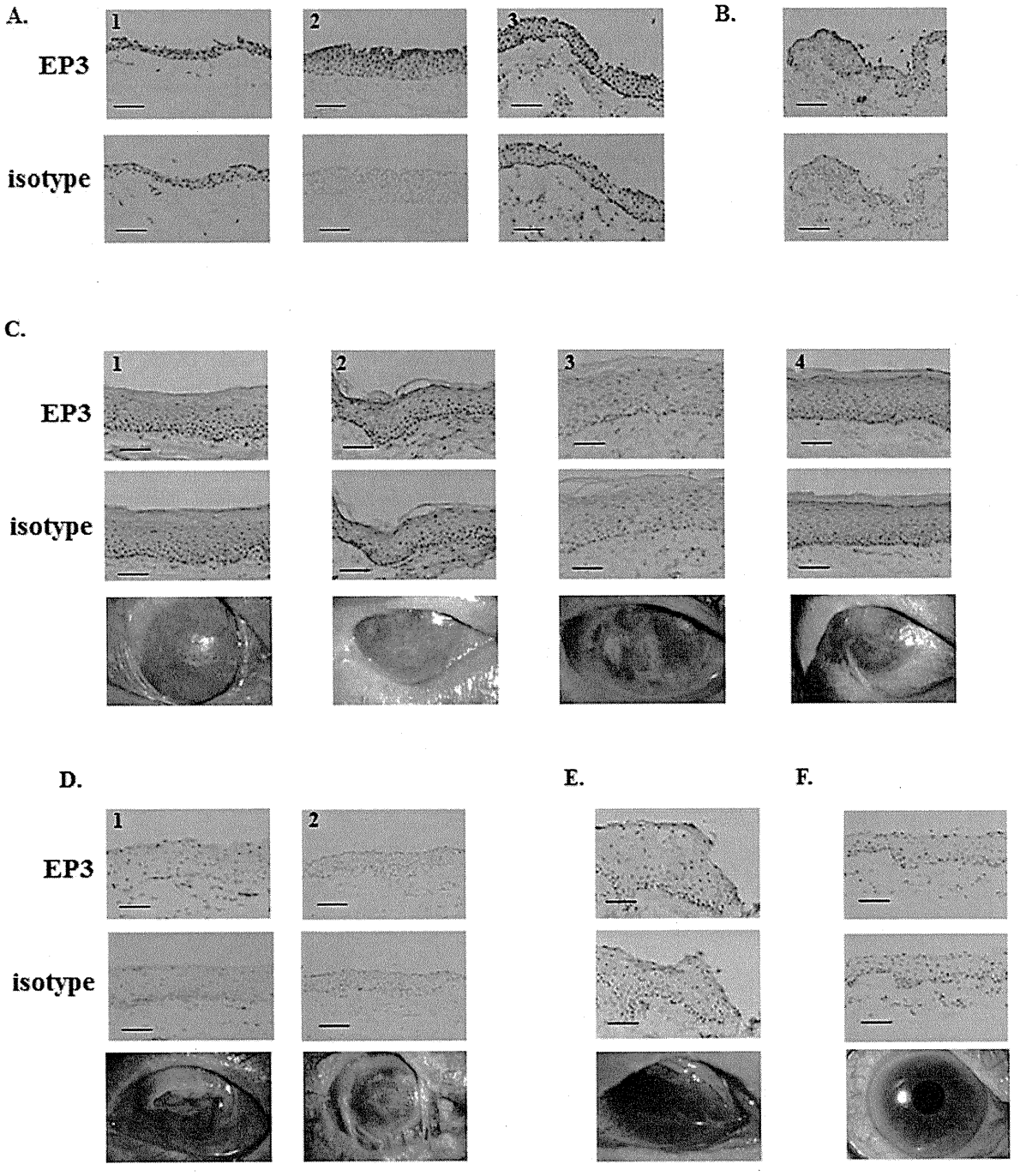

Figure 1. Immunohistological analysis of prostaglandin E receptor subtype EP3 in the conjunctival epithelium of the controls and SJS/TEN patients. A. Nearly normal conjunctival tissues from patients with conjunctivochalasis. B. Normal conjunctival tissue. C. Keratinized conjunctival tissues of SJS/TEN patients in the chronic stage. D. Non-keratinized conjunctival tissues of SJS/TEN patients in the sub-acute stage. E. Non-keratinized conjunctival tissues of SJS/TEN patients in the chronic stage. F. Visibly normal conjunctival tissue of an SJS/TEN patient with minor ocular sequelae (dry eye). C-F. The 3rd lane shows the ocular surface of SJS/TEN patients. Each scale bar represents a length of 100 μm.
doi:10.1371/journal.pone.0025209.g001

of human conjunctival epithelial cells, suggesting that EP3 in the conjunctival epithelium may down-regulate ocular surface inflammation [7].

In the current study we investigated the expression of EP3 protein in the conjunctiva of patients with various ocular surface diseases such as SJS/TEN, chemical eye burns, Mooren's ulcers, and ocular cicatricial pemphigoid (OCP).

Materials and Methods

Human conjunctival tissues

This study was approved by the Institutional Review Board of Kyoto Prefectural University of Medicine, Kyoto, Japan. All experiments were conducted in accordance with the principles set forth in the Helsinki Declaration.

Our immunohistochemistry controls were 3 nearly normal human conjunctival tissues acquired at surgery for conjunctivochalasis and one sample of normal conjunctival tissue acquired at limbal dermoid resection. Conjunctival tissues were also obtained from patients undergoing surgical reconstruction of the ocular surface due to SJS/TEN (n = 7), chemical eye burns (n = 3), OCP (n = 3), severe graft versus host disease (GVHD) (n = 1), pseudo-OCP (n = 1) and pterygium (PTG) (n = 1), from patients with Mooren's ulcers treated by resection of the inflammatory conjunctiva (n = 4), and from a patient with a giant papilla due to allergic vernal conjunctivitis. One conjunctival tissue sample was obtained from an SJS/TEN patient who did not require ocular surface reconstruction because ocular sequelae were minor (dry eye); this sample derived from additional unnecessary conjunctiva harvested just after cataract surgery.

Immunohistochemistry

For EP3 staining we used rabbit polyclonal antibody to EP3 (Cayman Chemical Co., Ann Arbor, MI) [3,6]. We previously checked and confirmed the EP3 specificity of this antibody using conjunctiva from EP3KO mice [6]. Further confirmation was by immunoblot analysis (Fig. S1). The secondary antibody (Biotin-SP-conjugated AffiniPure F(ab')$_2$ fragment donkey anti-rabbit IgG (H+L), 1:500 dilution; Jackson Immuno Research, Baltimore, MD) was applied for 30 min, then VECTASTAIN ABC reagent (Vector Laboratories, Inc., Burlingame, CA) was added for increased sensitivity with peroxidase substrate solution (DAB substrate kit; Vector) as a chromogenic substrate.

Evaluation of staining intensity using ImageJ software and down-regulation score

We converted the multi-color pictures into black and white pictures, and measured the gray value in the vertical line of the conjunctival epithelium. Then we recorded the average gray value on an intensity score from 5 to 16 (e.g. an average gray value of 100 was scored as 10). We also recorded the degree of down-regulation where "–" = intensity score 12–16, "+" = intensity score 8–11, and "++" = intensity score 5–7.

Results

As reported elsewhere [3], EP3 protein was detected in the nearly normal conjunctival epithelium from patients with conjunctivochalasis (Fig. 1A) and in the normal conjunctival

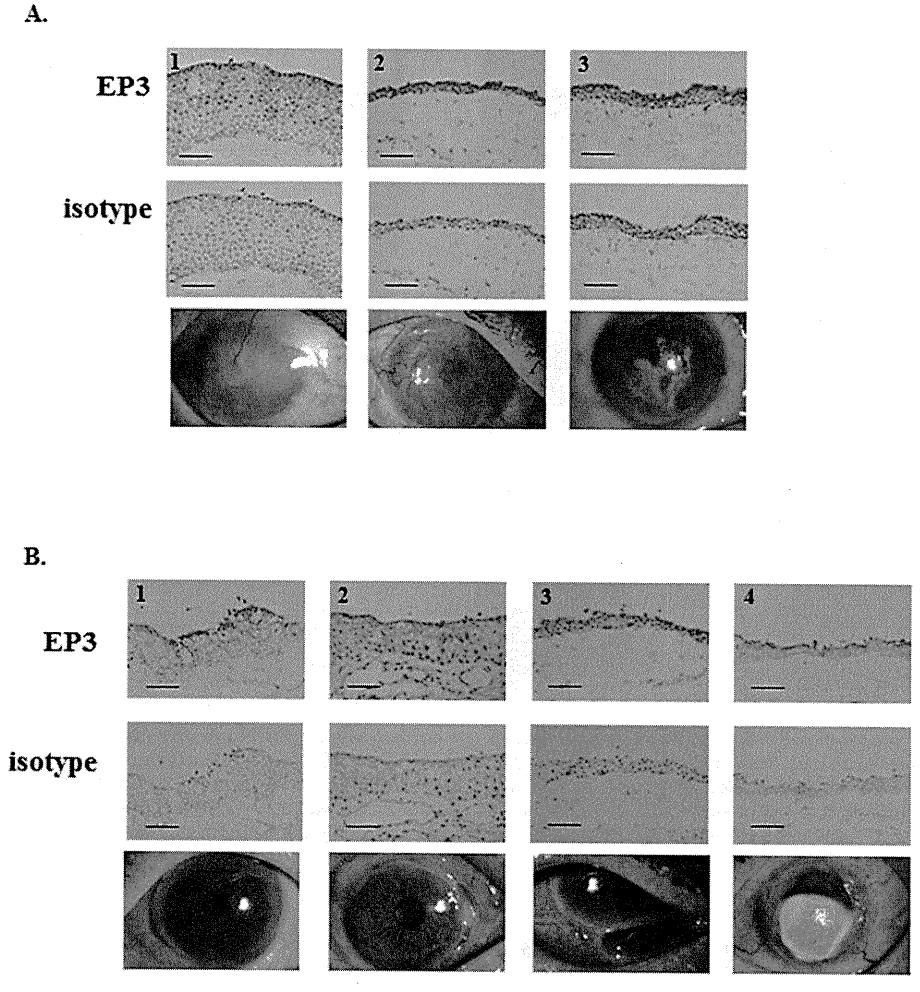

Figure 2. Immunohistological analysis of prostaglandin E receptor subtype EP3 in the conjunctival epithelium of patients with chemical eye burn and active Mooren's ulcer. A. Conjunctival tissues of patients with chemical eye burn requiring ocular surface reconstruction. B. Inflammatory conjunctival tissues of patients with active Mooren's ulcer requiring resection of the inflammatory conjunctiva. The 3rd lane shows the ocular surface of patients. Each scale bar represents a length of 100 μm.
doi:10.1371/journal.pone.0025209.g002

epithelium sample (Fig. 1B), but not in keratinized conjunctival epithelium from SJS/TEN patients in the chronic stage (Fig. 1C). When we examined non-keratinized conjunctival epithelium from SJS/TEN patients in the sub-acute- or chronic stage (Figs. 1D, 1E) we found that EP3 was markedly down-regulated. Interestingly, even in the conjunctival epithelium from the SJS/TEN patient manifesting only dry eye, EP3 was greatly down-regulated (Fig. 1F).

Comparison with conjunctival tissues from patients with chemical eye burn showed that although ocular surface findings were similar, EP3 protein was detected in the conjunctival epithelium of 3 patients with chemical eye burn as well as in control conjunctival epithelium from conjunctivochalasis patients (Fig. 2A). We also detected EP3 protein in conjunctival epithelium from 4 patients with Mooren's ulcer, however, it appeared to be somewhat down-regulated (Fig. 2B).

Next we examined conjunctival tissues from 3 patients with OCP; their ocular surface findings were very similar to those of SJS/TEN patients. No EP3 protein was detected in conjunctival epithelium from any of these patients (Fig. 3A), nor in conjunctival epithelium from a GVHD patient with severe conjunctival invasion to the cornea (Fig. 3B). When we assessed tissues from patients with pterygium (Fig. 3C), or pseudo-OCP (Fig. 3D), we detected EP3 protein in the conjunctival epithelium of pterygium patients as we did in the control conjunctival epithelium from a patient with conjunctivochalasis. EP3 protein was also present in conjunctival epithelium from patients with pseudo-OCP although it appeared to be slightly down-regulated. We also found EP3 protein in the conjunctival epithelium of a patient with giant papillae due to chronic allergic keratoconjunctivitis (Fig. 3E). In Table 1 we show the scores obtained by our evaluation of the staining intensity and degree of down-regulation for all samples.

We document that EP3 was expressed in conjunctival epithelium of patients with chemical eye burns and Mooren's ulcer and in normal human conjunctival epithelium. It was markedly down-regulated in the conjunctival epithelium of SJS/TEN- and OCP patients. Although we had only one patient each with severe GVHD, pterygium, pseudo-OCP, and chronic allergic keratoconjunctivitis, study of these samples suggested that EP3 is expressed in the conjunctival epithelium of patients with pterygium, pseudo-OCP, and chronic allergic keratoconjunctivitis, and that EP3 might be greatly down-regulated in the conjunctival epithelium of patients with severe GVHD.

Regarding in conjunctival epithelium, the expression of EP3 protein in the SJS/TEN and OCP patients was markedly decreased compared with normal conjunctiva. However, its expression in sub-conjunctival tissues may be up-regulated in

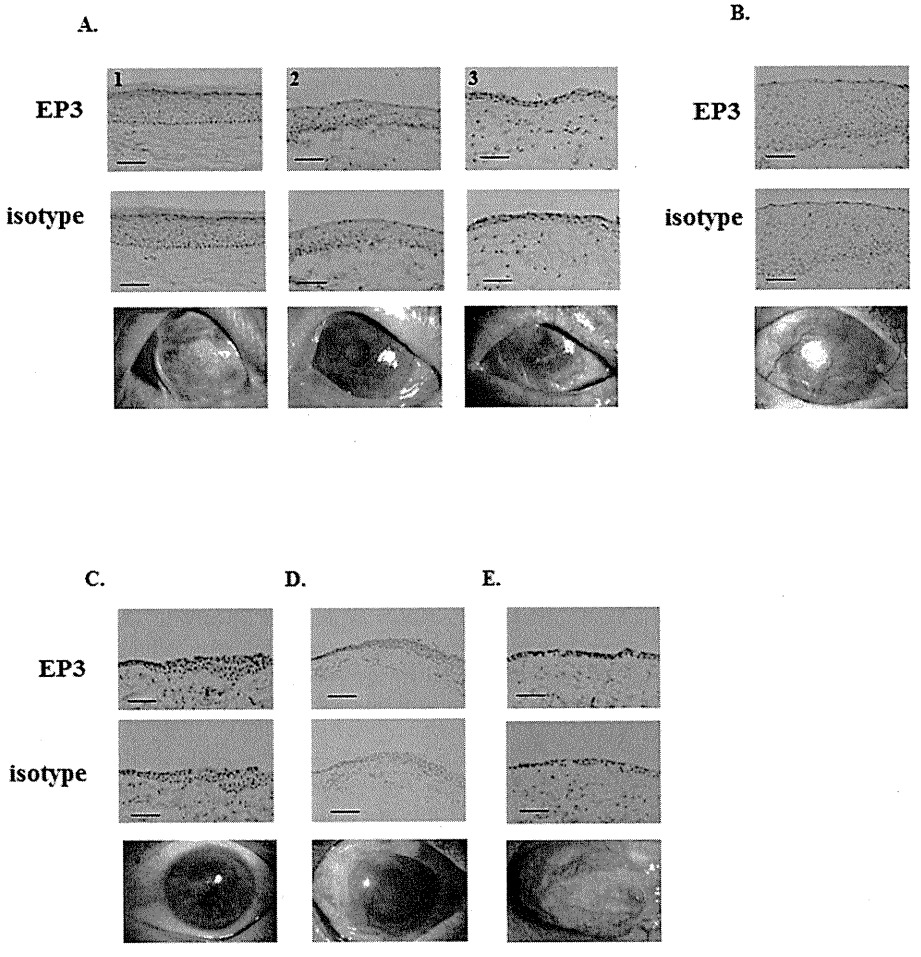

Figure 3. Immunohistological analysis of prostaglandin E receptor subtype EP3 in the conjunctival epithelium of patients with OCP (A), severe GVHD (B), pterygium (C), pseudo-OCP (D), and a giant papilla due to allergic vernal conjunctivitis (E). The 3rd lane shows the ocular surface of patients. Each scale bar represents a length of 100 μm.
doi:10.1371/journal.pone.0025209.g003

Table 1. Staining-intensity score of conjunctival epithelium.

Picture	Figure No	Intensity score	Down-regulation score	Disease
Figure 1	A1	14		Nearly normal conjunctival tissues from conjunctival chalasis
	A2	14		
	A3	14		
	B1	12		Normal conjunctival tissues
	C1	7	++	Keratinized conjunctival epithelium from SJS/TEN patients in the chronic stage
	C2	7	++	
	C3	6	++	
	C4	7	++	
	D1	5	++	Non-keratinized conjunctival epithelium from SJS/TEN patients in the sub-acute stage
	D2	5	++	
	E	5	++	Non-keratinized conjunctival epithelium from SJS/TEN patients in the chronic stage
	F	5	++	Conjunctival epithelium from an SJS/TEN patient manifesting only dry eye
Figure 2	A1	9	+	Chemical eye burn
	A2	16		
	A3	13		
	B1	12		Mooren's ulcer
	B2	12		
	B3	14		
	B4	10	+	
Figure 3	A1	6	++	Ocular cicatricial pemphigoid (OCP)
	A2	6	++	
	A3	6	++	
	B	6	++	GVHD with severe conjunctival invasion to the cornea
	C	13		Pterygium
	D	10	+	Pseudo-OCP
	E	16		Chronic allergic keratoconjunctivitis

doi:10.1371/journal.pone.0025209.t001

some instances because vascular endothelia expressing the EP3 protein could be increased due to the presence of inflammatory infiltrating cells in sub-conjunctival tissues (Fig. S2).

Discussion

We previously reported that in Japanese SJS/TEN patients there was a significant association between severe ocular surface complications and prostaglandin E receptor 3 gene (*PTGER3*) polymorphisms and that compared to the controls, EP3 expression was greatly reduced in their conjunctival epithelium [3]. Here we studied keratinized and non-keratinized conjunctival epithelia of SJS/TEN patients and the conjunctival epithelium of an SJS/TEN patient whose ocular sequelae were minor (dry eye). We found that EP3 was markedly down-regulated not only in keratinized- but also in non-keratinized conjunctival epithelia and even in the normal conjunctiva of a patient in the chronic stage of SJS whose only ocular sequela was dry eye. Our results suggest that the strong down-regulation of EP3 in conjunctival epithelium of SJS/TEN patients is associated with the pathogenesis and pathology of the disease because PTGER3 (EP3) polymorphisms are significantly associated with SJS/TEN.

Severe chemical eye burn results in conjunctival invasion into the cornea due to a deficiency in corneal epithelial stem cells; this leads to devastating ocular surface disorders similar to SJS/TEN. However, EP3 was not down-regulated in the conjunctival epithelium of patients with severe chemical eye burns, suggesting that the pathology of the ocular surface changes was not associated with EP3 expression.

In patients with Mooren's ulcer the peripheral stroma is destroyed first circumferentially then centrally, resulting in the characteristic overhanging inner edge. This is an inflammatory disease of the ocular surface that may require resection of the inflammatory conjunctiva adjacent to the ulcer. We found that the conjunctival epithelium of the inflammatory conjunctival tissues adjacent to the ulcer clearly expressed EP3 protein, indicating that other factors besides inflammation are required for a marked down-regulation of EP3 expression.

OCP is a subset of mucous membrane pemphigoid. It is characterized by the abnormal production of circulating autoantibodies directed against various components of the basement membrane zone and the generation of proinflammatory and fibrogenic cytokines [8]. We found that, as in SJS/TEN patients, EP3 was markedly down-regulated in the conjunctival epithelium of OCP patients with conjunctival invasion to the cornea. As in OCP patients, we failed to detect EP3 protein in the conjunctival epithelium of a patient with severe GVHD with conjunctival invasion to the cornea. This suggests that in a common mechanism(s) may underlie the pathology of SJS/TEN and OCP, especially in ocular surface epithelium such as the conjunctival epithelium. EP3 expression has been reported in skin and PGE_2 was produced abundantly during skin allergic

inflammation [5], suggesting that there is no association between decreased EP3 expression and the increased production of cornified proteins in SJS/TEN and OCP.

We found that EP3 was clearly expressed in the conjunctival epithelium of our patients with pterygium, pseudo-OCP, and a giant papilla of allergic vernal conjunctivitis. Interestingly, the expression of EP3 in conjunctival epithelium from patients with OCP and pseudo-OCP was different: EP3 was clearly present in the patient with pseudo-OCP but not the patient with OCP. The patient with pseudo-OCP had received long-term treatment with eye drops for glaucoma; this resulted in a deficiency of corneal epithelial stem cells and led to conjunctival invasion into the cornea. This suggests that different mechanisms are involved in the expression of EP3. We also detected EP3 in the conjunctival epithelium of the patient with allergic vernal conjunctivitis. Elsewhere we documented that PGE_2 acts as a ligand for EP3 in the conjunctival epithelium and down-regulates the progression of murine experimental allergic conjunctivitis [6]. Although EP3 may down-regulate allergic reactions in patients with allergic conjunctivitis, its loss may not be a causative factor.

In summary, EP3 is expressed not only in normal human conjunctival epithelium but also in the conjunctival epithelium of patients with chemical eye burns and Mooren's ulcer. On the other hand, it is markedly down-regulated in the conjunctival epithelium of SJS/TEN- and OCP patients.

Supporting Information

Figure S1 The rabbit polyclonal antibody to EP3 we used is checked and confirmed the EP3 specificity of this antibody using immunoblot analysis.
(TIF)

Figure S2 EP3 expression in sub-conjunctival tissues in a SJS/TEN patient in the chronic stage. In some instances of SJS/TEN patients, vascular endothelia expressing the EP3 protein are found.
(TIF)

Author Contributions

Conceived and designed the experiments: MU. Performed the experiments: MU. Analyzed the data: MU. Contributed reagents/materials/analysis tools: CS NY TI SK. Wrote the paper: MU.

References

1. Matsuoka T, Narumiya S (2007) Prostaglandin receptor signaling in disease. Scientific World Journal 7: 1329–47.
2. Sotozono C, Ueta M, Koizumi N, Inatomi T, Shirakata Y, et al. (2009) Diagnosis and treatment of Stevens-Johnson syndrome and toxic epidermal necrolysis with ocular complications. Ophthalmol 116: 685–90.
3. Ueta M, Sotozono C, Nakano M, Taniguchi T, Yagi T, et al. (2010) Association between prostaglandin E receptor 3 polymorphisms and Stevens-Johnson syndrome identified by means of a genome-wide association study. J Allergy Clin Immunol 126:1218-25 e10.
4. Kunikata T, Yamane H, Segi E, Matsuoka T, Sugimoto Y, et al. (2005) Suppression of allergic inflammation by the prostaglandin E receptor subtype EP3. Nat Immunol 6: 524–31.
5. Honda T, Matsuoka T, Ueta M, Kabashima K, Miyachi Y, et al. (2009) Prostaglandin E(2)-EP(3) signaling suppresses skin inflammation in murine contact hypersensitivity. J Allergy Clin Immunol 124: 809–18 e2.
6. Ueta M, Matsuoka T, Narumiya S, Kinoshita S (2009) Prostaglandin E receptor subtype EP3 in conjunctival epithelium regulates late-phase reaction of experimental allergic conjunctivitis. J Allergy Clin Immunol 123: 466–71.
7. Ueta M, Matsuoka T, Yokoi N, Kinoshita S (2011) Prostaglandin E2 suppresses polyinosine-polycytidylic acid (polyI:C)-stimulated cytokine production via prostaglandin E2 receptor (EP) 2 and 3 in human conjunctival epithelial cells. Br J Ophthalmol 95: 859–63.
8. Razzaque MS, Foster CS, Ahmed AR (2003) Role of connective tissue growth factor in the pathogenesis of conjunctival scarring in ocular cicatricial pemphigoid. Invest Ophthalmol Vis Sci 44: 1998–2003.

Mathematical Projection Model of Visual Loss Due to Fuchs Corneal Dystrophy

Shin Hatou,[1] Shigeto Shimmura,[1] Jun Shimazaki,[2] Tomohiko Usui,[3] Shiro Amano,[3] Hideaki Yokogawa,[4] Akira Kobayashi,[4] Xiaodong Zheng,[5] Atsushi Shiraishi,[5] Yuichi Ohashi,[5] Tsutomu Inatomi,[6] and Kazuo Tsubota[1]

Purpose. To devise a mathematical disease classification model for eyes with primary guttata cornea, on the bases of endothelial loss trajectory and probability of advanced disease.

Methods. A series of 1971 patients (3281 eyes), some with and some without guttata corneas, undergoing specular microscopy were retrospectively reviewed. The eyes were classified into four stages; stage 0, without guttae; 1, guttata cornea without edema; 2, mild Fuchs' corneal dystrophy (FCD); and 3, severe FCD, according to clinical records, and patient age and corneal endothelial cell density (ECD) were plotted. Nonparametric density smoothing was used to create a contour map, and a best-fit curve for ECD loss was calculated. The relation between ECD decrease rate and the stages were evaluated.

Results. Endothelial decrease rate in stage 0 was 0.44%/year, which was compatible with that of normal eyes reported in previous studies. Decrease rates of stages 1, 2, and 3 were 0.81%, 2.65%, and 3.08%/ year, respectively. The age-ECD loss curves of 1.40%/year ($ECO_{1.4}$) and 2.00%/year ($ECO_{2.0}$) further divided stage 1 into three subgroups; stage 1a, asymptomatic guttata cornea; 1b, borderline guttata cornea; and 1c, pre-FCD. The $ECO_{2.0}$ cutoff line differentiated eyes with FCD from those without edema with a sensitivity and specificity of >90%. Stage 1c eyes were below $ECO_{2.0}$ and had a decrease rate as high as FCD.

Conclusions. This mathematical model can be used to predict the prognosis of patients with primary guttata cornea. (*Invest Ophthalmol Vis Sci.* 2011;52:7888-7893) DOI:10.1167/iovs.11-8040

From the [1]Department of Ophthalmology, Keio University School of Medicine, Shinjuku, Japan; the [2]Department of Ophthalmology, Tokyo Dental College Ichikawa General Hospital, Tokyo, Japan; the [3]Department of Ophthalmology, Tokyo University School of Medicine, Tokyo, Japan; the [4]Department of Ophthalmology, Kanazawa University School of Medicine, Kanazawa, Japan. the [5]Department of Ophthalmology, Ehime University School of Medicine, Matsuyama, Japan; and the [6]Department of Ophthalmology, Kyoto Prefectural University of Medicine, Kyoto, Japan.

Supported by a grant from the Ministry of Health, Labor and Welfare, Japan. The sponsor or funding organization had no role in the design or conduct of this research.

Submitted for publication June 14, 2011; revised August 8, 2011; accepted August 12, 2011.

Disclosure: **S. Hatou**, None; **S. Shimmura**, None; **J. Shimazaki**, None; **T. Usui**, None; **S. Amano**, None; **H. Yokogawa**, None; **A. Kobayashi**, None; **X. Zheng**, None; **A. Shiraishi**, None; **Y. Ohashi**, None; **T. Inatomi**, None; **K. Tsubota**, None

Corresponding author: Shigeto Shimmura, Department of Ophthalmology, Keio University School of Medicine, 35 Shinanomachi, Shinjuku, Tokyo 160-8582, Japan;shige@sc.itc.keio.ac.jp.

Fuchs' corneal dystrophy (FCD) is a progressive, bilateral corneal dystrophy.[1] There is a progressive loss of corneal endothelial cells with secretion of an abnormally thickened basement membrane, leading to corneal guttae formation.[1] On specular microscopy, these corneal guttae are observed as dark areas.[1,2] As endothelial function deteriorates, corneal edema increases and visual acuity declines,[2] and FCD is a major indication for keratoplasty (corneal transplants) in the United States.[3-5] Although FCD is recognized as a dominantly inherited disorder, females are predisposed to it and develop corneal guttae 2.5 times more frequently than do males, progressing to corneal edema 5.7 times more often than do males.[6] The prevalence of primary guttata cornea and FCD are lower in Japan than in the United States.[7,8] This difference in prevalence is thought to be mainly attributable to the racial difference.[7]

Primary guttata cornea is believed to be a preliminary stage of FCD. Krachmer et al.[6] graded guttata cornea and FCD according to a spread of guttae and reported that there was a positive correlation between age and grade of guttae. However, the exact natural course of guttata cornea, or whether all cases of guttata cornea progress to FCD remains to be determined. A prospective study that follows the decline in endothelial cells density (ECD) with age would be ideal for predicting the natural course of guttata cornea; however, a very long follow-up would be required, and recruiting asymptomatic potential patients is practically impossible, especially in Japan. A retrospective study with a large database and an adequate mathematical model can be used in a similar way to predict the prognosis of patients with guttata cornea. In this report, we retrospectively reviewed age and ECD in a large group of hospital-based patients and evaluated the prevalence of guttae, male:female ratio, and distribution of age and ECD. In addition, we propose a new classification of guttata cornea based on a mathematical model that adequately predicts the prognosis of disease.

Methods

Subjects

Clinical records of outpatients who underwent specular microscopy for corneal endothelial cell counts from January through December 2009 in six hospitals affiliated with the Fuchs' Corneal Dystrophy Study Group of Japan were retrospectively reviewed. The purpose of specular microscopy for those patients were routine examination before ocular surgery, follow-up for corneal diseases that were thought to have little effect on endothelium (such as keratoconus or lattice corneal dystrophy), or follow-up for diagnosed Fuchs' corneal dystrophy. Patients who had a history of trauma, corneal infection, intraocular inflammation, intraocular surgery, or laser iridotomy were excluded from the study. Endothelial photographs were taken at the center of the pupillary area with a noncontact specular microscope (Nonkon Robo F & A; Konan Medical, Nishinomiya, Japan, or EM-3000; Tomey,

Investigative Ophthalmology & Visual Science, October 2011, Vol. 52, No. 11

Nagoya, Japan), and analyses of the photographs were performed with an automatic cell analysis system attached to the microscope. Data concerning patient age, sex, presence of guttae, and ECD were recorded. The eyes were classified into four groups by slit lamp examination according to modified Stocker's classification[9]:

Stage 1: Guttata cornea without the stroma or the epithelium being affected

Stage 2: Permeation of corneal stroma with fluid, edema of epithelium, and bullae formation

Stage 3: Late stages with subepithelial connective tissue formation, vascularization, and scar formation

Other eyes without corneal guttae were classified as stage 0. During the rest of the article, the term Fuchs' corneal dystrophy (FCD) represents stage 2 and 3, since eyes in these stages have symptoms related to corneal edema. The study complied with the Declaration of Helsinki. Approval was granted by the Committee for the Protection of Human Subjects of each hospital.

Mathematical Model of Endothelial Cell Loss Rate

To construct a mathematical model of decrease in endothelial cells, we made the following two assumptions:

1. The ECD at 5 years of age is 3600 cells/mm^2. This is common to all classes.
2. From 5 years of age, the decrease rate (percent/year) of ECD is constant in each class, but different between classes.

Murphy et al.[10] reported that during first 2 years of life ECD decreased rapidly because of corneal growth, and after that the decrease rate slows down to 0.56%/year. The effect of corneal growth on ECD ends at 5 years of age or earlier. To simplify our mathematical model, we assumed that ECD at 5 years of age was common to all classes and regarded this point as the base point of age-ECD curve in our mathematical model. Because the onset of FCD is in adulthood, we believe that this assumption is acceptable. We substituted the mean ECD of normal 5-year-old children (3600 cells/mm^2) in the report of Nucci et al.[11] for the base point. We assumed that the (percentage) decrease rate is dependent on the class, and it is constant in each class from 5 years of age. Based on these assumptions, the following differential equation stands:

$$dE_{(t)}/d(t) = -(D/100) \cdot E_{(t)}$$

$$E_{(t=0)} = 3600$$

where t is age 5 years; $E_{(t)}$ is endothelial cell density at t years (in cells per square millimeter); and D is the decrease rate (percent).

The solution to the differential equation is the following:

$$E_{(t)} = 3600e^{[-(D/100)t]}$$

Using this mathematical model, an age-ECD curve in each class can be drawn by the least-squares method. An age–ECD curve of optimal decrease rate can be drawn as well.

Statistical Analysis

Scatterplotting, analysis of variance (ANOVA), nonparametric density smoothing, age-ECD curve, and other statistical analyses were calculated by or written in commercial software (Excel 2007; Microsoft, Redmond, WA, and JMP 8 software; SAS, Cary, NC). $P < 0.05$ was considered statistically significant.

Results

Characteristics of Patients

Age, sex, and stage of reviewed patients and eyes are presented in Table 1. The prevalence of guttata cornea (stage 1+2+3) was 12.73%. The prevalence of stage 1 was 10.65%, and FCD (stage 2+3) was 2.08%. The male: female ratio in each stage was as follows; 1: 1.03 (stage 0), 1: 1.88 (stage 1), 1: 2.43 (stage 2), and 1: 4.67 (stage 3). Females were more predisposed to stage 1 or FCD than males, and the ratio increased in advanced stages.

Age-ECD Curve of 2.0% Differentiates Fuchs' Dystrophy

Figure 1, left shows the scatterplot between age and ECD for each stage. Nonparametric density smoothing was drawn on the scatterplot (Fig. 1, right), which represents the contour of plot density. The age-ECD curves based on our mathematical model were drawn by the least-squares method. Table 2 shows ECD with sample sizes at 5-year intervals for grades 0 to 3, which enables the mean ECD data of grade 0 to 3 to be compared at various ages.

The decreased rate curve of stage 1 age-ECD was 0.81%, which was closer to that of stage 0 (decrease rate, 0.44%) than that of stage 2 (2.65%) or stage 3 (3.08%). The decrease rate of stage 0 in our study was 0.44%, which is within the range of

Table 1. The Age, Sex, and Stages of Reviewed Patients and Eyes

Patient Stage	Age, y (Mean ± SD)	Male (*n*)	Female (*n*)	Total (*n*)	Prevalence (%) Total	Male	Female
0	65.3 ± 16.2	848	872	1720			
1	68.5 ± 14.3	73	137	210	10.65	7.84	13.17
2	70.3 ± 10.6	7	17	24	1.22] 2.08	0.75] 1.07	1.63] 2.98
3	75.1 ± 12.4	3	14	17	0.86]	0.32]	1.35]
Total	66.6 ± 15.4	931	1040	1971	12.73	8.91	16.15

Eye Stage	Male (*n*)	Female (*n*)	Total (*n*)
0	1426	1483	2909
1	103	205	308
2	13	28	41
3	5	18	23
Total	1547	1734	3281

Prevalence of FCD was calculated as sum of stage 2 and 3. In this table, if a patient had eyes in different stages, then he or she was classified in the severer of the stages between the eyes.